METEOROLOGICAL OFFICE
12 JUN1978
C
LIBRARY

MET O 11 TECHNICAL NOTE No. 102

# THE MET O 11 FOUR-DIMENSIONAL DATA ASSIMILATION SCHEME: PILOT EXPERIMENT

R H MARYON

Met O 11 (Forecasting Research Branch)
Meteorological Office
London Road
Bracknell
Berkshire

September 1977

NB. This paper has not been published. Permission to quote from it should be obtained from the Assistant Director of the above Meteorological Office branch.

CONTENTS


1. THEORETICAL BACKGROUND

1.1 Introduction

1.2 Optimum Interpolation: basic formulation

1.3 Ill-conditioning

2. EXPERIMENTAL DETAILS

2.1 Introduction

2.2 Outline of Met O 11 data assimilation scheme

2.3 The background field

2.4 Interpolation in the vertical

2.5 Quality control

2.6 Adjustment of the wind field

2.7 Modification of the divergence field

2.8 Selection of observations and final stages

3. RESULTS OF EXPERIMENT OF 30th DECEMBER 1975

3.1 Synoptic situation

3.2 The operational forecast

3.3 The assimilated forecasts to 12Z, 30th Dec., 1975

3.4 Initialization or Assimilation?

3.5 Forecasts to midnight, 31st Dec., 1975

4. CONCLUSIONS

4.1 General

4.2 The optimum interpolation scheme

4.3 Quality control scheme

4.4 Modification of the updated fields

References

Appendix 1. A. Variances and covariances of model error

B. Treatment of observations and observational error

Appendix 2. Alternative vertical interpolation scheme.

Appendix 3. Treatment of friction at 1000 mb

Appendix 4. Alternative methods of modifying the divergence field

Figures

SUPPLEMENT The experiment of 29th March 1977

MET O 11 FOUR-DIMENSIONAL DATA ASSIMILATION SCHEME

PILOT EXPERIMENT

## 1. Theoretical Background

### 1.1 Introduction

We require of a method of objective analysis that it should utilize both forecast field values and fresh data, making due allowance for the statistical relation between the forecast and analysed fields and for observational error, so that more weight is given to reliable data than to data considered inaccurate. The scheme should also incorporate quality control which is so structured that it becomes less stringent in areas where new observations are sparse. All of these requirements are met by the regression technique known as optimum interpolation which, insofar as it has been applied to meteorological data, was pioneered by the Russians, notably L.S. Gandin. The method has attracted increased attention in Britain in recent years, for instance in the analysis scheme for GATE.

It is also desirable that a scheme of analysis should be capable of assimilating off-time data, if only at discrete intervals, in order to utilize the wealth of satellite and aircraft reports now available as well as synoptic data for intermediate hours. Hence the term "four-dimensional".

The present experiment was set up to look at the feasibility of linking a four-dimensional optimum interpolation assimilation scheme to U.K. objective analysis requirements, and to form some initial comparisons with the present operational procedures.

To summarise the current procedure very briefly, new data arriving at Bracknell are subjected to an initial processing which excludes that failing certain quality controls, and stores acceptable data in the Basic Analysis Datasets (BADS). An objective analysis of the geopotential fields is carried out for 00Z and 12Z using the BADS and values drawn from a background field, by means of an orthogonal polynomial fitting technique /7/. The background field in low latitudes is derived from an updated version of the previous analysis, while elsewhere a 12 hour forecast therefrom is utilized. The next step, initialization, derives the wind field from the mass field via the balance equation and 12, 24 etc hour forecasts can then be made /4/. The procedure is illustrated in fig 4.2.

There are a number of disadvantages inherent in the operational procedure as it stands. Firstly, little (objective) use is made of off-time data, which includes a great deal of valuable material. Secondly the derivation of the winds from the height field every 12 hours results in much useful information being lost. Finally, the criticism has been made of polynomial interpolation methods in general

(e.g. Gandin, /8/) that although a weighting may be given to an observation according to an estimation of its reliability, no explicit reference is made to the statistical properties of the fields of the elements being analysed. Four-dimensional data assimilation using optimum interpolation may enable us to overcome these drawbacks to some extent.

1.2 Optimum Interpolation: Basic formulation

A brief outline of the now standard formulation is given. More detailed accounts may be found in Belousov, Gandin and Mashkovich, /1/, from whom I have borrowed freely, and in the classical text by Gandin, the "Objective Analysis of Meteorological Fields".

Set out in its simplest form the objective analysis problem is to approximate the value of an element, f, at a grid-point, $l$, using a linear combination of values $f_i$ of the element at n nearby observing stations:

$$f_l^I = \sum_{i=1}^{n} q_i f_i^O \qquad (1)$$

where the $q_i$ are weights, superscript I refers to the interpolated value, O to that observed.

In a manner analogous to the usual techniques of regression we may minimise the mean square of the interpolation error at grid-point $l$ over a period:

$$\overline{E_l^2} = \overline{(f_l^I - f_l)^2} \qquad (2)$$

(where $f_l$ represents the true value) by substituting for $f_l^I$ from (1) and applying the condition for extremum

$$\frac{\partial \overline{E^2}}{\partial q_k} = 0 \quad , \quad k = 1, 2, \ldots n$$

This yields a system of equations for the regression coefficients $q_i$:

$$\sum_{i=1}^{n} \overline{f_i^O f_j^O} q_i = \overline{f_j^O f_l} \quad , \quad j = 1, 2, \ldots n \qquad (3)$$

Estimation of the meaned products is of doubtful feasibility, and it is necessary to derive a more practicable formulation for (3).

In the method of optimum interpolation the values of an element can be represented as the sum of its normal or climatological value and the deviation from the norm. In practice, however, it is more convenient and more appropriate for day-to-day meteorological analysis to consider the deviations from a forecast background value $f^B$. The deviation at a grid-point may then be interpolated in a manner analogous to (1):

$$(f_l^I - f_l^B) = \sum_{i=1}^{n} q_i (f_i^O - f_i^B) \qquad (4)$$

where it is understood the $q_i$ form a different set to those of equation (1). This will yield a set of equations for the coefficients

$$\sum_{i=1}^{n} \overline{(f_i^O - f_i^B)(f_j^O - f_j^B)}\, q_i = \overline{(f_j^O - f_j^B)(f_l - f_l^B)}, \qquad j = 1, 2, \ldots n \qquad (5)$$

The observed values will, in general, differ from the "true value" and may be represented

$$f_i^O = f_i + \epsilon_i \qquad (6)$$

where $f_i$ is the true value at the point of observation and $\epsilon_i$ the observational error. If it is assumed that the observational errors are random in the horizontal and are uncorrelated with the values of f at any point we have

$$\overline{\epsilon_i \epsilon_j} = 0 \qquad (7)$$

$$\overline{\epsilon_i (f_j - f_j^B)} = 0 \qquad (8)$$

so that (5) may be expressed

$$\sum_{i=1}^{n} \overline{(f_i - f_i^B)(f_j - f_j^B)}\, q_i + \overline{\epsilon_j^2} q_j = \overline{(f_j - f_j^B)(f_l - f_l^B)}, \qquad j = 1, 2, \ldots n \qquad (9)$$

Now this offers a practicable scheme, as the

$$\overline{(f_i - f_i^B)(f_j - f_j^B)} = m_{ij}, \qquad \text{say,}$$

the meaned products of the deviations of the actual values from the forecast at i and j, are covariances diagnostic of the structure of model error which may be estimated from the processing of past data.

In practice it is found that for meteorological fields the value of the covariance is dependent upon the distance between the points: the $(f_i - f_i^B)$, $(f_j - f_j^B)$ will have a low correlation if i, j are sufficiently far apart, while $m_{ij}$ reduces to the model error variance if i and j coincide. If isotropy and homogeneity of the field are assumed, covariance would depend solely on the distance between points, and the $m_{ij}$, $m_{jl}$ might be ascertained from some function F of that distance:

$$m_{ij} = F\left(\sqrt{(x_i - x_j)^2 + (y_i - y_j)^2}\right) \qquad (10)$$

These assumptions hold to a fair degree of approximation over limited areas for most important meteorological elements, but not over distances in excess of a few hundred kilometres. However the assumptions are believed not to be restrictive for analysis by optimum interpolation as long as a good estimate of the statistical structure of the error field can be obtained.

One approach to the problem is to norm the covariance function $m_{ij}$ to form the autocorrelation function $\mu_{ij}$

$$\mu_{ij}(r) = \frac{\overline{(f_i - f_i^B)(f_j - f_j^B)}}{\sqrt{\overline{(f_i - f_i^B)^2} \cdot \overline{(f_j - f_j^B)^2}}} \qquad (11)$$

where r represents the distance between the points i, j, and $\mu$ takes values between +1 and -1. Studies have shown that the normed function satisfies the isotropic and homogeneous assumptions reasonably well for distances between points of up to about 2000 km. In practice, then, we determine the correlation function $\mu$ by some empirical means, compute the denominator in equation 11 from past forecasts and hence obtain an estimate of the covariance function $m_{ij}$ for utilizing in the optimum interpolation scheme.

Estimates of the observational error variances $\overline{\epsilon_j^2}$ required for insertion in equation 9 may be computed both from past observed and analysed data and from published tables of instrumental accuracy.

The error of the interpolation is given by

$$E_l^2 = \overline{(f_l - f_l^B)^2} - \sum_{i=1}^{n} q_i \overline{(f_i - f_i^B)(f_l - f_l^B)} \qquad (12)$$

1.3. Ill-conditioning

Consider a linear combination of deviations of an element from background value:

$$L = \sum_{i=1}^{n} q_i (f_i - f_i^B)$$

We may write down the mean square taken over a quantity of data such as might be utilized in the processing of past forecasts

$$\overline{L^2} = \sum_{i=1}^{n} \sum_{j=1}^{n} \overline{(f_i - f_i^B)(f_j - f_j^B)}\, q_i q_j$$

which is clearly positive for all $q_i$, $q_j$. The implication is that the covariance matrix for

$$\overline{(f_i - f_i^B)(f_j - f_j^B)}$$

which is used in the solution of the system of equations for determining the coefficients $q_i$, (equation 9), is positive definite. This is equivalent to saying that the $\mu_{ij}(r)$ (equation 11) must have a positive definite matrix, a condition usually attained in practice as the empirically derived correlations will approximate functions of positive error spectrum /1/. In the solution of system (9) the matrix is perturbed by the inclusion of the observational error covariances, the effects of which become perhaps rather more significant in the case of interpolation in the vertical. (Section 2.4).

Further problems may arise with the conditioning of the system. If two reporting stations lie very close together their data are strongly correlated, and accordingly each station should attract a smaller weight than an isolated station at about the same distance from the grid point being fitted. Theoretically this is allowed for automatically in optimum interpolation /1/, but it was found in practice /6/ that the linear equations for the weights could become ill-conditioned under these circumstances, especially if the grid-point and the two neighbouring stations lie in a straight line.

The method adopted in the present experiment to counter this was similar to that devised for the GATE analysis: where two reports were found to lie in close proximity the observations (or more precisely their deviations from background) and the corresponding grid-coordinates were averaged, and an appropriately reduced error variance allocated. Observations treated in this manner have been designated "superobs".

In this way as well as solving the problem of ill-conditioning we also optimise the use we are able to make of the available data. In addition, the problem of spatial error correlation of nearby stations due to sub-grid-scale effects, which runs counter to the basic assumptions of optimum interpolation, does not arise /6/.

## 2. Experimental Details

### 2.1 Introduction

Although optimum interpolation can be applied in three dimensions, and even extended so that, for example, wind observations are utilized in the analysis of the height field /2/ it was decided that for the present experiment a fairly straightforward formulation would be adhered to: no attempt was made to update a field using information derived from different elements, while vertical and horizontal interpolations were confined to separate steps. Vertical interpolation, in fact, was carried out only at observation points as a preliminary to a subsequent horizontal analysis at the model grid-points.

The new data utilized in the updating procedure consisted of winds and heights derived from synoptic reports from land stations and ships, radio-sonde and radar-wind reports and AIREPS. Programming to accommodate satellite data such as GOES winds and SIRS heights was also carried out although the actual assimilation of GOES data was left to a subsequent experiment.

The main stages of the experiment may be summarised:

1. Using the ØØZ main run analysis for 30th December 1975 as a starting point, forecasts were run to T+3, T+6, T+9, T+12 hours to form a control. After an operational type analysis and initialization at 12Z, a further forecast was made to T+24 hours, along the lines of the usual main run (Fig 4.2).

2. Starting with the same ØØZ analysis, assimilated forecasts were run up to T+12 hours, the fields being updated at T+3, T+6 and T+9 hours by observations made on or about that time. Separate updating runs using (a) height, (b) wind (c) height+wind data were performed. Following (a) and (c) analysis, initialization, and a forecast to T+24 hours were carried out, as in 1 (Fig 4.4).

3. The combined assimilation of heights and winds was carried through so as to include the operational T+12 data. Then a forecast to T+24 was run without prior initialization (Fig 4.3).

### 2.2 Outline of Met O 11 Data Assimilation Scheme

The following scheme was used to assimilate non-synoptic and off-time data into the model fields of geopotential and wind:

Height Update:

1. Extraction of data from height BADS, followed by vertical interpolation of data from observed to model levels. The background field necessary to the interpolation was provided by a forecast height field.

2. Horizontal analysis to the grid-points using optimum interpolation, again with the forecast field as the background. Doubtful data was excluded by quality control routines.

3. The wind field is then adjusted to restore balance with the height field.

4. A forecast to the next assimilation time.

Wind Update:

5. Extraction of data from wind BADS, followed by vertical interpolation from observed to model levels. The background field was provided by the forecast wind field.

6. A horizontal wind analysis using optimum interpolation with the same background field, and incorporating quality control.

7. An adjustment to the wind field to suppress spurious divergences resulting from the preceding steps which might lead to unwanted gravity waves in

8. A forecast to the next assimilation time.

Height + Wind Update:

To carry out the combined height and wind update it was only necessary to follow steps 1 to 8 (excluding step 4). The background field for steps 5 and 6 is then the adjusted wind field from step 3.

A number of these steps will be looked at in greater detail in the ensuing paragraphs.

## 2.3 The Background Field

The basic equation (4) requires the value of the background field at the point of observation. This value was obtained from the forecast values at the model grid-points by a bi-linear interpolation in the horizontal, followed if necessary by an interpolation in the vertical from model levels to observation levels.

The linear interpolation is straightforward:

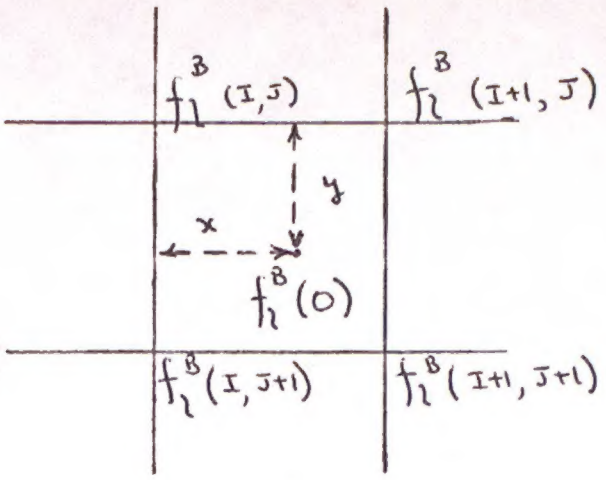


Fig 2.1

We deduce
$$f_l^B(0) = (1-y)(1-x)f_l^B(I,J) + x(1-y)f_l^B(I+1,J) + y(1-x)f_l^B(I,J+1) + xy f_l^B(I+1,J+1)$$

where the $f_l^B(I,J)$ etc, are the background values at the four neighbouring grid-points, $f_l^B(0)$ the required value at the point of observation.

For reports from sondes at 150, 250, 850 mb and from AIREPS, etc, the interpolation from model levels to that of the observation took the usual Lagrangian formulation: for an observation level p, given the background values $f^B$ at model levels $p_i$, $i = 1, 2, \ldots n$

$$f^B(p) = \sum_{i=1}^{n} L_i(p) f^B(p_i)$$

where $L_i(p)$ is the Lagrange multiplier function

$$L_i(p) = \prod_{\substack{j=1 \\ j\neq i}}^{n} (p-p_j) \Big/ \prod_{\substack{j=1 \\ j\neq i}}^{n} (p_i-p_j)$$

For background values of the field at 150 and 250 mb and for AIREPS, a 4-point fitting to the 100, 200, 300 and 400 mb model levels was used; to derive the 850 mb value a 5-point fitting to 600, 700, 800, 900, 1000 mb data. $\mathrm{Log}_n p$ was used instead of p, as tests made against the ICAO atmosphere showed that it yielded superior results.

## 2.4 Interpolation in the Vertical

A version of optimum interpolation was used to interpolate (or extrapolate) to the model levels from the observation at any particular locality, and in some cases this might be a surface report. Errors in the geopotential height as measured by radio-sonde are usually taken to be correlated amongst themselves in the vertical. Under these circumstances equation (7) does not hold, and the linear system for

determining the coefficients must be written

$$\sum_{i=1}^{n}\left[\overline{(h_i-h_i^B)(h_j-h_j^B)}+\overline{\epsilon_i\epsilon_j}\right]q_i=\overline{(h_j-h_j^B)(h_l-h_l^B)} \qquad (13)$$
$$j=1,2,\ldots n$$

where i, j now refer to observed levels. Expression (12) for interpolation error is not affected. The radar winds were regarded as uncorrelated in the vertical, so that no such adjustment would be required.

The schemes represented by (9) and (13), where, of course, the $q_i$ are now the coefficients of the winds or heights reported for the levels i of a sounding, proved to give unrealistic values for some of the coefficients, notably those applied to 1000 and 100 mb. Where observed values used in an optimum interpolation lie in a straight line, the nearer data should so screen that further from the point of interpolation that the outlying data is given a very low weighting (assuming that the quality of the observations is roughly equal). In fact, it was found that the weights computed for the data at the extremities of the vertical soundings were too large. The reason for this is not clear. During the objective analysis of the GATE experiment it was found that the linear system of equations for the coefficients $q_i$ could become ill-conditioned under the circumstances outlined in section 1.3. It is possible that the properties of the solution matrix are in some way sensitive to the particular structure of the observational error covariances over the 10 model levels; these augment the model covariances in the solution matrix (equation 13).

However this may be it was decided that for the current experiment, instead of minimising the mean square interpolation error (equation 2), the following quantity should be minimised instead:

$$\overline{E_l^2}=\overline{(h_l^I-h_l^O)^2} \qquad (14)$$

where $h_l^O$ represents a hypothetical observed value at a level l. This leads to an equation for the $q_i$ coefficients of the form

$$\sum_{i=1}^{n}\left[\overline{(h_i-h_i^B)(h_j-h_j^B)}+\overline{\epsilon_i\epsilon_j}\right]q_i=\overline{(h_j-h_j^B)(h_l-h_l^B)}+\overline{\epsilon_j\epsilon_l} \qquad (15)$$
$$j=1,2,\ldots n$$

with the interpolation error given by

$$E_l^2=\overline{(h_l-h_l^B)^2}-\sum_{i=1}^{n}q_i\left[\overline{(h_i-h_i^B)(h_l-h_l^B)}-\overline{\epsilon_i\epsilon_l}\right] \qquad (16)$$

The foregoing applies to sonde heights; for the winds, which are treated as uncorrelated in the vertical we have the analogous expressions

$$\sum_{i=1}^{n} \overline{(u_i - u_i^B)(u_j - u_j^B)} q_i + \overline{\epsilon_j^2} q_j = \overline{(u_j - u_j^B)(u_l - u_l^B)} \qquad (17)$$

$$j = 1, 2, \ldots n, \text{ but } j \neq l$$

and

$$\sum_{i=1}^{n} \overline{(u_i - u_i^B)(u_l - u_l^B)} q_i + \overline{\epsilon_l^2} q_l = \overline{(u_l - u_l^B)^2} + \overline{\epsilon_l^2} \qquad (18)$$

$$\text{where } j = l$$

with the error given by

$$E_l^2 = \overline{(u_l - u_l^B)^2} - \sum_{i=1}^{n} q_i \overline{(u_i - u_i^B)(u_l - u_l^B)} + \overline{\epsilon_l^2} q_l \qquad (19)$$

Examination of the augmented matrices for systems (15), (17), and (18) shows that if l is, in fact, an observation level,

$$q_l = 1, \quad q_j = 0 \quad (j \neq l)$$

and accordingly, from (16) or (19)

$$E_l^2 = \overline{\epsilon_l^2}$$

i.e. the interpolated value at level l is the same as the value observed. This is not the same as optimum interpolation proper which would use even an observation at the point of interpolation in linear combination with other data. The revised scheme essentially fits the observations, where they are available, allowing their errors to be handled in the subsequent (horizontal) interpolation. At model levels for which observational data is <u>not</u> available it will be noted that, for winds, equation (18) and the last term of (19) became redundant, so that the equations revert to the original formulations in (9) and (12).

Aware of the shortcomings of this method (what, for instance, is to be understood by (14)?) Cattle has outlined a scheme (Appendix 2) which treats the observations as though they are perfect in the vertical interpolation, and for which the terms involving $\overline{\epsilon_i \epsilon_j}$ appear only in the expression for interpolation error.

For AIREPS and GOES data it is possible to use the standard optimum interpolation technique, adapted for a single reported level. Thus if the report is at level i, and vertical interpolation is to be made to level l, we have for the u-component of the wind

$$u_l^I = u_l^B + q(u_i^O - u_i^B) \qquad (20)$$

where q is obtained from

$$\left[\overline{(u_i - u_i^B)^2} + \overline{\epsilon_i^2}\right] q = \overline{(u_i - u_i^B)(u_l - u_l^B)} \qquad (21)$$

(of equations (4) and (9)),
with an error

$$E_l^2 = \overline{(u_l - u_l^B)^2} - q\,\overline{(u_i - u_i^B)(u_l - u_l^B)} \qquad (22)$$

It was decided that optimum interpolation would not be appropriate for the vertical interpolation of SIRS heights. The treatment of SIPS and other modes of observation will be looked at from a practical angle in Appendix 1.

At the end of the vertical interpolation the processed data is passed, with the estimates of error, to the horizontal analysis. The data transmitted is in the form

[observed (or interpolated) minus background] value,

ready for direct insertion into the horizontal interpolation.

2.5 Quality Control

Following vertical interpolation to the model levels a horizontal interpolation to the model grid-points was made using a suitable selection of adjacent observations, the standard techniques of optimum interpolation being employed.

Prior to the actual insertion of the new data each observation (or vertical interpolation) is subjected to quality control. This takes the following form:

(i) The observation is checked against the background field. That is, having calculated $|f^O - f^B|$ where f = u, v or h, we test to see whether

$$|f^O - f^B| > 2\sqrt{\epsilon_O^2 + \epsilon_B^2} \qquad (23)$$

where $\epsilon_O^2$ is the variance of the observational error and $\epsilon_B^2$ is the variance of the background (forecast) error.

This preliminary test is incorporated as a sort of sieve, in order to reduce the computational load incurred by the next step:

(ii) Observations satisfying (23) fail the test against the background and are further tested against other adjacent observations. The scheme used is similar to that devised for the GATE analysis (and was also recommended by Gandin, 1968). An interpolated value at the point of observation, $f^c$, is calculated in the usual optimum interpolation manner, which also provides a measure of the interpolation error $\epsilon_c^2$ at that point. The observation is rejected if it differs from the interpolated value by an amount proportional to the size of the combined interpolation and observational error; that is, if

$$|f^c - f^o| > 3\sqrt{\epsilon_o^2 + \epsilon_c^2} \qquad (24)$$

(For the maximum likelihood derivation of this test see Appendix 2 of /6/). Test (24) automatically ensures that observations in regions of sparse data are more readily accepted than those where data is plentiful (and the interpolation error $\epsilon_c^2$ smaller as a result).

For computational convenience we test

$$\left[\sum_{i=1}^{n} q_i (f_i^o - f_i^B) - (f^o - f^B)\right]^2 > q(\epsilon_o^2 + \epsilon_c^2) \qquad (25)$$

where the $f_i^o$ are the set of adjacent observations; reference to equation (4) will demonstrate the equivalence of (24) and (25). Observations satisfying (25) are then rejected.

(iii) The effect of rejecting observations at the end of step (ii) is perhaps to delete a report already utilized in previous tests (25). This is tidied up to some extent by retesting in a second sweep all the observations satisfying (23) and rejecting any additional observations satisfying (25). This procedure could be improved upon, and requires some revision.

## 2.6 Adjustment of the Wind Field

Following the horizontal analysis of the geopotential it is necessary to adjust the winds in order to restore the balance of the wind and mass fields. This was done by adding a geostrophic wind increment (reflecting the changes in geopotential) to the values of the forecast wind:

$$\underline{V}^A = \underline{V}^F + g/f \, \underline{k} \times \nabla (h^u - h^F) \qquad (26)$$

where superscripts F, U, A relate to the forecast, updated and adjusted fields.

A finite-difference representation of (26) was applied to the model levels 900-100 mb. At 1000 mb an adjustment for friction was incorporated which took the form outlined in Appendix 3.

2.7 Modification of the Divergence Field

This adjustment follows the horizontal interpolation which updates a wind field. Insertion of unbalanced wind data leads to the propagation of gravity waves in the subsequent forecast step. This is because spurious divergences (and hence vertical velocities) are then imposed on the model fields, although a degree of smoothing is probably achieved as a result of the optimum interpolation.

A good deal of preliminary work was directed towards the mitigation of these effects. Initially an attempt was made to reduce unwanted modes by selectively damping the divergence field by the application of Sadourney diffusion. These experiments were inconclusive, and later investigations were aimed more towards modifying the divergence by adjusting the velocity components immediately after the wind update. Several methods of accomplishing this were considered. The method adopted made use of the fact that the horizontal wind components, u, v, may be resolved into a divergent and a rotational component:

$$(u, v) = (u_D + u_R, v_D + v_R)$$

or what is equivalent

$$\underline{V} = \nabla\phi + \nabla \times \psi \qquad (27)$$

where $\phi$ is the velocity potential, $\psi$ the stream function. The aim was to replace the updated divergence field by the original (forecast) divergence, while the updated vorticity is left unchanged. This does not in any way balance the wind and mass fields but simply gives realistic values of the divergence at the cost of losing part of the new wind information. This combination of wind update followed by the restoration of the original divergence field could conveniently be described as a "vorticity update".

Now from (27) $\nabla . \underline{V} = \nabla^2\phi$

or $$\nabla^2\phi = D, \qquad (28)$$

the horizontal divergence.

If we calculate

$$D_F = \frac{\partial v_F}{\partial y} + \frac{\partial u_F}{\partial x} \qquad \text{(forecast divergence)}$$

$$D_u = \frac{\partial v_u}{\partial y} + \frac{\partial u_u}{\partial x} \qquad \text{(updated divergence)} \qquad - (29)$$

we may introduce velocity potentials which satisfy

$$\nabla^2 \phi_F = D_F \,, \quad \nabla^2 \phi_u = D_u$$

But $$\nabla^2 (\phi_F - \phi_u) = D_F - D_u$$

We therefore solve

$$\nabla^2 \bar{\phi} = \bar{D} \qquad (30)$$

the bar representing difference, with boundary condition

$$\frac{\partial \bar{\phi}}{\partial n} = 0 \qquad (31)$$

where n is normal to the boundary, as there is no updating around the edge of the octagon.

Upon the solution of (30) subject to (31) we increment the updated velocity field by

$$\delta u = \frac{\partial \bar{\phi}}{\partial x} \,, \quad \delta v = \frac{\partial \bar{\phi}}{\partial y} \,.$$

Poisson's equation (30) was solved by Gauss-Seidel successive over-relaxation using standard finite difference techniques. Convergence was in general slow, the best results being obtained from acceleration parameters between 1.91 and 1.97 depending on the precise formulation. The convergence criterion chosen was that

$$|\bar{\phi}^{(m+1)} - \bar{\phi}^{(m)}| < 10^{-4} |\bar{\phi}^{(m)} + \varepsilon|$$

over the whole grid, $\varepsilon$ being set at $2.0 \times 10^5$.

Two further methods were considered. The first (Washington and Baumhefner, /16/) was to modify the updated divergence field so that the vertically averaged divergence over any column of the model is approximately zero. This removes any

excess of divergence, but has the disadvantage of modifying the entire divergence field, even where no update has been carried out. The second was similar, but modified the divergence field so that the vertically averaged divergence over any column of the model is the same as the original (forecast) vertically averaged divergence. This would have the effect of preserving divergence where no update has taken place, but it is not certain that the method would damp gravity waves elsewhere. Further details of these methods will be found in Appendix 4.

2.8 Selection of Observations and Final Stages

To avoid ambiguity it will be as well to reiterate that it is the deviation of observations from background value that is used in optimum interpolation. Words such as observation, report, height or wind in this section must be interpreted in this sense.

To carry out the updating of a grid-point it is necessary to make a selection from the surrounding observations, and consideration has to be given to the number, type and horizontal distribution of the reports to be utilized. The general consensus of published papers on optimum interpolation appears to favour a choice of about 8 neighbouring stations. More stations would increase the computational load and the dangers of ill-conditioning without materially improving the analysis. Rather fewer stations would be acceptable provided they were uniformly distributed around the grid-point - an ideal which is by no means consistently attained.

In practice we may expect to find a random scatter of observations around each grid-point which will be of varying quality, and many of which may well be interpolated values following the vertical interpolation of sonde ascents, etc, to model levels. This presents the considerable programming problem of conducting a search for the 8 most effective stations in the most economical way.

For the present experiment it was decided to scan only those reports situated within 5 grid-lengths of the grid-point being updated. To facilitate this the octagon levels were each divided into 169 squares of side 5 grid-lengths. The observations were then sorted into the various squares or "blocks", and a block-directory of observations set up. For each grid-point in turn a cluster of up to 9 blocks is scanned: that in which the point lies and the 8 contiguous, or as many as are within, or partly within, the octagon boundary (Fig 2.2). Each report, provided it lies within the limiting distance, is then allocated to its appropriate quadrant as illustrated in Fig 2.3

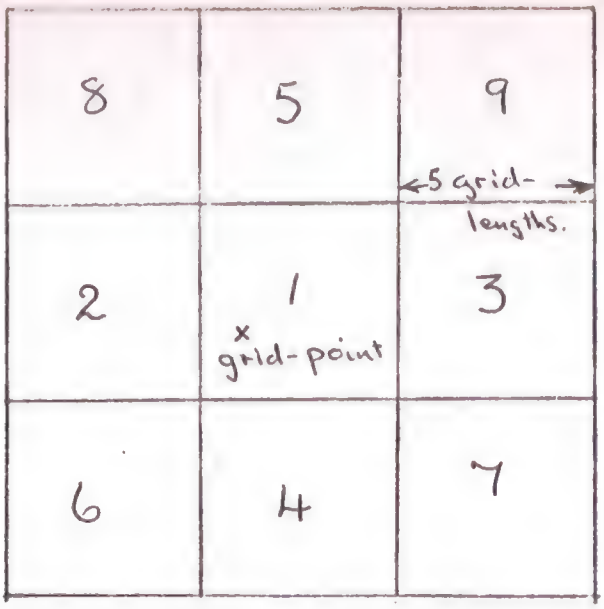


Fig 2.2

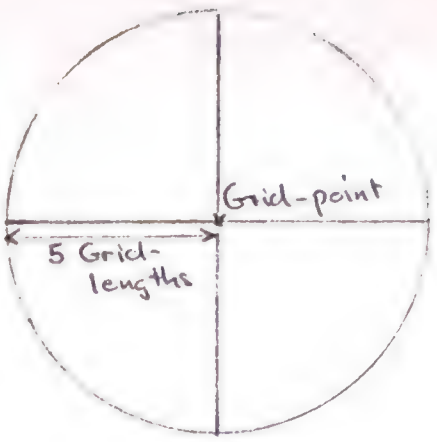


Fig 2.3

Showing (arbitrary) order of scansion of blocks around a grid-point and the quadrants to which the observations are allocated.

Observed or interpolated values to be used in the optimum interpolation were then chosen according to the following scheme:

1. Pick out the nearest two radio-sonde heights or radar winds in each quadrant.

2. If necessary make up to two in each quadrant by accepting observations of any type, or interpolations from radio-sonde data, which would have the largest weighting in the absence of any other reports.

Now equation (9) adapted for a single observation gives

$$\left[\overline{(f_i - f_i^B)^2} + \bar{\epsilon}_i^2\right] q = \overline{(f_i - f_i^B)(f_g - f_g^B)}$$

where the subscript g refers to a value at a grid-point.

Substitution from equation (11) yields, for a single observation

$$\left[\overline{(f_i - f_i^B)^2} + \bar{\epsilon}_i^2\right] q = \mu_{ig}(r)\,\overline{(f_i - f_i^B)^2}$$

which is re-arranged

$$q = \frac{\mu_{ig}(r)}{1 + \dfrac{\bar{\epsilon}_i^2}{\overline{(f_i - f_i^B)^2}}} \qquad (39)$$

to provide the measure of the weighting. It will be noted that this test takes into account the quality of an observation as well as its proximity to the grid-point.

3. If necessary, the total of 8 reports is made up irrespective of quadrant by taking observations of any type, or interpolations from sonde, utilising (32) as before. A maximum of 6 observations is permitted under this head.

4. If the total is still less than 8, step 2 is repeated accepting values interpolated from data other than radio-sondes.

5. If the total is still less than 8, step 3 is repeated accepting values interpolated from data from sources other than radio-sonde.

When, for each grid-point, a suitable selection of observations has been made the covariances $\overline{(f_i-f_i^B)(f_j-f_j^B)}$ and regression coefficients $q_i$ are computed. Although a scan for stations in close proximity is made at an earlier stage of the processing, a final check is made so that unwarrantably large coefficients resulting from a poorly conditioned system (9) may be identified and dealt with via the "superobbing" procedure.

Finally the grid-point is updated using the background value and the linear combination of observed deviations from background:

$$f_1^I = f_1^B + \sum_{i=1}^{n} q_i (f_i^O - f_i^B)$$

In fig 2.4 is a listing of the subroutines involved in the final stages of the wind update. This summarises the foregoing and incidentally shows the scope of the programming required merely to update the grid-points.

An account of the estimation of the variances and covariances of model error, and of the treatment of the various types of observation and observational error will be found in Appendix 1.

| SUBROUTINE | INVOKED BY | PURPOSE |
|---|---|---|
| FBLOCK | MAIN-LINE PROG. | Set up a block-directory of observations (Section 2.8) |
| UVCHECK | MAIN-LINE PROG. | Quality-control of observations (Section 2.5) |
| UVSCAN | MAIN-LINE PROG. | I/O of grid-points; invokation of sub-routines for remaining stages |
| OBLIST | UVSCAN or UVCHECK | Selection of observations for each grid-point (Section 2.8) or of neighbouring reports for obs. undergoing quality control. |
| MATRIX | UVSCAN or UVCHECK | Compute model covariances and $q_i$ for selected observations. |
| WEIGHT, SOLVE | MATRIX | Accesory routines to solve systems of linear equations |
| ILLCON | UVSCAN or UVCHECK | Identification of large $q_i$ and correction of ill-conditioning. |
| SORTOB, SHUFFL | OBLIST | Accessory sorting routines |

Fig 2.4 Final stages of the wind update

## 3. Results of Experiment of 30th December 1975

### 3.1 Synoptic Situation

Fig 3.1 presents the main run analysis for midnight on 30th December 1975, which formed the starting point for the various assimilation experiments, and fig 3.3 the operational update run analysis for 12Z. A deep depression just east of Iceland is moving ENE towards the Norwegian Coast. By 12Z the low had covered about half the distance and had deepened from 962 mb to below 956 mb. Further south over the Atlantic, between about 20 and 40 deg N, is a slack area of low pressure which by 12Z shows two distinct centres on hand-analysed charts.

Pressure remains generally high over Central Europe and the Mediterranean, and also down the eastern seaboard of America. A high cell in the region of the Azores is weakening slowly, while a slack low persists near the Canaries.

### 3.2 The Operational Forecast

The 12 hour operational forecast (Fig 3.2) from the midnight main run analysis may be compared to Fig 3.3. The forecast is evidently quite a good one. Most of the features just described are slightly less pronounced in terms of central pressure, while one or two elsewhere are over-accentuated - the North Russian low for example. The most obvious failing is in the treatment of the Central Atlantic low complex.

### 3.3 The Assimilated Forecasts to 12Z, 30/12/75

The effects of assimilating height data, wind data and both height+wind data at 03, 06 and 09Z, and carrying the forecast through to 12Z may be seen in Figs 3.4, 3.5 and 3.6 respectively. These may be compared to the operational forecast (Fig 3.2) and the verifying analysis (Fig 3.3). The height update is superior to the operational forecast in its handling of almost every major feature. The more realistic appearance of the mid-Atlantic low will be observed. Compared with the analysis, the high over S Europe and the Mediterranean is over-accentuated, however.

The wind update shows an improvement over the operational forecast in places, but lacks the overall superiority of the height assimilation. Over the eastern Atlantic, for instance, it is poor. The treatment of the S European high is creditable.

Like the height assimilation, the combined height+wind update is superior to the operational forecast. The two assimilations were carefully compared with a hand-analysed chart for 12Z, and it proved difficult to choose between them. Broadly speaking the height update tended to handle the sea areas better, the combined update the land. The problem in the latter case may lie in the many ship winds which

go into the assimilation. An update run which omitted the 06 and 09Z ship reports did, in fact, go part of the way towards correcting the worst shortcomings of the wind-only assimilation over sea areas.

Compared with the surface, upper air features are less well-defined while the difference between the various forecasts are not always easy to assess by eye from contour charts (see, for example, Figs 3.7 to 3.10). Accordingly, the root-mean-square of the height error over the octagon of the various runs as compared with the verifying analysis was calculated for each model level. The results are presented graphically in Fig 3.11 which shows how well the height and the combined update runs compare with the operational T+12 forecast. Below 600 mb the position is particularly satisfactory; above that level the combined update (the best at low levels) deteriorates slowly until by 100 mb it is inferior to both the wind update and the operational forecast. Caution is necessary in assessing results from these statistics. The differences between the forecasts are often small, while a slight horizontal displacement of an otherwise well forecast feature might have a significant impact on the RMS error. The good performance of the operational forecast at high levels may be explained in part by its relationship to the background field of the verifying analysis.

Statistics confined to mid-latitudes (Atlantic sector) show RMS errors as low as 13 m at the surface for the height and combined updates, and a creditable performance by the wind update at AIREP levels (300 mb). Here again, incorporation of winds to produce a combined update led to poor results at high levels.

## 3.4 Initialization or Assimilation?

At this stage of the experiment objective analysis at 12Z was carried out using as background fields both the operational 12-hour forecast and the height and combined assimilation runs. For all of this work 12Z data available for the operational main run were used. The analysis was followed by the usual initialization. It was at once apparent that the process of analysis at T+12 largely rendered any earlier updating redundant. Whether the background field was provided by the operational forecast or by one of the superior assimilated forecasts the end product (e.g. Figs 3.12, 3.13) was much the same. The updating does make a positive contribution here and there, but over large areas of the charts it is difficult to discern any significant difference.

A combined height+wind update using the 12Z data, following the assimilated forecast to T+12 was also carried out in order to make comparisons with the conventional analyses. Reference to the hand-drawn chart for 12Z revealed a first-rate analysis (Fig 3.14). Attention is drawn to the complex low in mid-Atlantic,

which is at last adequately handled, while many other features are treated very well. Here and there the conventional analysis and initialization compare with some advantage, but overall there is no doubt that the update is superior.

### 3.5 Forecasts to Midnight, 31st December 1975

An important test, clearly, would be the 12-hour forecasts from midday on the 30th, using as a start dataset the various initializations and the 12Z updated assimilation.

As might be expected, the forecasts based on the initializations all proved to be extremely similar (e.g. Fig 3.15); that based upon the 12Z update is shown in Fig 3.16. A careful comparison of these forecasts with the subjectively analysed chart for midnight yielded no clearcut verdict. A failing of the assimilated forecast, a retardation of the movement of the Scandinavian low, will be referred to in Section 4.3

There is less ambiguity about the RMS height error over the octagon (Fig 3.17; comparisons were made with the ØØZ operational update-run analysis). This shows the forecast from the assimilation to have less error throughout the 10 model levels. This must be considered an encouraging result, although it would be unwise to draw general conclusions from a single experiment.

## 4. Conclusions

4.1 The four-dimensional data assimilation scheme utilized quickly outstripped the operational forecast in overall accuracy, so that by T+12 a superior background field was available for the conventional analysis and initialization procedures. The effect of these procedures however was to render much of the additional input information redundant in areas where a reasonable quantity of new T+12 data was available. It seems questionable whether it would be worthwhile carrying out the whole updating procedure (and a great deal of computing is involved) merely to produce a background chart. Much of the additional information would be lost except on the rare occasions where, for some reason, little main-hour data is available. If a better background field were considered desirable to contribute to an improved analysis in regions of sparse data, considerable computing time could be saved and little accuracy lost by confining the update to height data only.

Where analysis and initialization were eschewed and the T+12 data assimilated using the same optimum interpolation techniques as for the earlier updates, a superior forecast to T+24 was obtained in this instance in terms of RMS error, although examination of the principal synoptic features was inconclusive.

Assimilation of wind data to produce a combined height+wind update failed to yield any consistent improvement in the RMS height error over the straight height update. Individual surface features could be found which were treated better by the combined update, particularly over land. Some of its shortcomings over sea areas may be attributed to assimilation of large numbers of ship winds of varying pertinence to the 1000 mb flow.

4.2 The Optimum Interpolation Scheme

An attractive feature of optimum interpolation is that it copes very well with irregularly distributed data and with data obtained from different types of instrumental system - an advantage over some alternative techniques. The fundamental idea behind the method is that, with the proviso that fresh data belong to the populations for which the error variances have been ascertained, the resultant interpolation will on average be the best.

Due to the occurrence of data-sparse areas automatic methods of analysis require a forecast background field, with the result that there is usually a degree of smoothing of the new data towards the configuration of the background. This is all to the good where there are large quantities of data of moderate or variable quality, and it is such data that optimum interpolation is best geared to handle. The extent of the smoothing will depend on the relative sizes of the error attributable to the background field and to new observations. This, incidentally, easily provides for "bogusing" by the allocation of an arbitrarily low error (as in the GATE analysis, for example).

It is possible that the model errors vary in different geographical locations; for example a particular region may exhibit a bias at a certain time of year. In addition the covariance of model errors is strongly time-dependent as the accuracy of forecast fields falls off with time. Allowance for such effects, were they sufficiently understood, could be incorporated into the scheme via the covariance matrices (equation 11) but at the cost of increased complexity. Some work by Bengtsson and Gustavsson, incidentally, /3/, suggests that the autocorrelation function $\mu_{ij}$ is only weakly time-dependent.

The application of optimum interpolation to the vertical was satisfactory: an estimate of interpolation error is easily computed and passed to the next stage of horizontal analysis, while it is a convenient method of extrapolating a single report such as an AIREP to several levels. For upper air soundings for which values at observation levels are forced to the actual height reported (Section 2.3) the economy of substituting a simpler (polynomial) method of interpolation to missing levels merits consideration.

4.3 Quality Control Scheme

Although the exclusion of gross error by an automatic quality control routine is straightforward, to differentiate between the "maverick" and the good observation that represents a new and considerable departure from the background field is notoriously difficult. The scheme described in Section 2.5 worked quite well although some good observations were, in fact, excluded. In one instance, for example, the passage of a front at a weather ship resulted in a veer of surface wind which the quality control would not accept. An investigation was made into the rejection of some 300 mb winds at 06Z on 30/12/75, when a jet core was aligned SW-NE over Northern Scotland. It was apparent that the preliminary test against background (equation 23) having no dependence upon wind strength, was more likely to exclude extreme winds (120 kt was observed at Stornoway). In addition, as the observations were in the jet core, the second test against surrounding reports (equation 24) involved almost without exception weaker winds. These observations were also rejected at 12Z, a fact which doubtless contributed to the retardation apparent in the movement of the North Atlantic low during the forecast based upon the 12Z assimilation.

4.4 Modification of the Updated Fields

On the limited evidence to hand it seems that the balancing of the wind field (section 2.6) and the modification of the divergence field (section 2.7) have the effect of containing the generation of spurious waves unless a large quantity of new data is assimilated at one time, when some initial oscillations in the subsequent forecast become apparent. If such oscillations become sufficiently pronounced, the background field forecast for the next assimilation (i.e. after 3 hours) might be affected. In this case some form of suppression may need to be imposed using techniques such as dynamical initialization or damped integration.

Fig 4.1 illustrates typical fluctuations in a spot value of surface pressure in the course of forecasts made with and without preliminary application of the various types of divergence adjustment outlined at the end of section 2.7. In this instance not a great quantity of fresh data had been assimilated, and the success of these adjustments in damping the variation is apparent.

Figs 4.2 to 4.4 give a diagrammatic representation of the analysis and forecast cycles used operationally and in the course of this experiment.

Some preliminary results of a second experiment, together with some observations of particular relevance to section 4.4 above are annexed as a supplement.

ACKNOWLEDGEMENT

This Technical Note collates the work of the Met O 11 data assimilation group. Papers and memoranda by Dr H Cattle and Dr A Dickinson were drawn from freely. Most of the initial computer programming was carried out by Mr C S Clarke.

REFERENCES


1. Belousov, S.L., Gandin, L.S. and Mashkovich, S.A., Computer processing of meteorological data. Leningrad, Gidrometeoizdat, 1968.

2. Bengtsson, L. 4-dimensional assimilation of meteorological observations. GARP Publications Series, No. 15, 1975.

3. Bengtsson, L. and Gustavsson, N., An experiment in the assimilation of data in dynamical analysis. Tellus XXIII, 1971.

4. Benwell, G.R.R., Gadd, A.J., Keers, J.F., Timpson Margaret S., White, P.W., The Bushby-Timpson 10-level model on a fine mesh. Met Office Scientific Paper No. 32, 1971.

5. Cattle, H., Data assimilation experiments with the Met Office 10-level model. GARP program on numerical experimentation, Report No. 11, 1976.

6. Cattle, H. et al., A scheme for the objective analysis of GATE data. Met O 11 Technical Note No. 74, 1976

7. Dixon, R., The three-dimensional analysis of meteorological data. Met Office Scientific Paper No. 31, 1970.

8. Gandin, L.S., Objective analysis of meteorological fields. Leningrad, Gidrometeoizdat, 1963.

9. Hawson, C.L. and Caton, P.G.F., A synoptic method for the international comparison of geopotential observations. Met Mag 90, 1073,1961.

10. Jones, D.E., The United Kingdom Meteorological Office objective analysis scheme for GATE. Met Mag 105, 1250, 1976.

11. Lewis, J.M. and Grayson, T.H., The adjustment of surface wind and pressure by Sasalei's Variational matching technique. 1972.

12. Rutherford, I.D., Experiments on the updating of primitive equation forecasts with real wind and geopotential data. Third conf., Probability and Statistics, Boulder, Colorado, American Met Soc, 1973.

13. Rutherford, I.D., Data assimilation by statistical interpolation of forecast error fields. Journal Atmos. Sci 29. 1972.

14. Singleton, F., Human intervention in the operational objective analysis. Met Mag 104, 1240, 1975.

15. Spackman, L.A., Compatibility and performance of radio-sonde measurements of geopotential height in the lower stratosphere - 1976. Met O 20 Technical Note No. II/106.

16. Washington, W.M. and Baumhefner, D.P., A method of removing Lamb waves from initial data for primitive equation models. Jnl Applied Met Vol 14 No. 1, 1975.

APPENDIX 1

A. VARIANCES AND COVARIANCES OF MODEL ERROR

Vertical Interpolation Rearranging equation(11)we have

$$\overline{(f_i - f_i^B)(f_j - f_j^B)} = \left[\overline{(f_i - f_i^B)^2}\right]^{1/2}\left[\overline{(f_j - f_j^B)^2}\right]^{1/2} \mu_{ij}(Z) \qquad (33)$$

Values for the $\overline{(f_i - f_i^B)^2}$ may be obtained by processing past data. Table A1 shows the values used in the experiment.

| P mb | 100 | 150 | 200 | 250 | 300 | 400 | 500 | 600 | 700 | 800 | 850 | 900 | 1000 |
|---|---|---|---|---|---|---|---|---|---|---|---|---|---|
| $(h-h^B)^2(m^2)$ | 1313 | 1333 | 1327 | 1290 | 2213 | 832 | 582 | 455 | 385 | 353 | 352 | 359 | 376 |
| $\begin{Bmatrix} u-u^B \\ v-v^B \end{Bmatrix}^2 {}_2(ms^{-1})^2$ | 18.6 | 26.2 | 31.7 | 35.7 | 38.3 | 27.4 | 19.3 | 15.3 | 13.1 | 12.3 | 12.6 | 13.1 | 14.7 |

Table A1: Variances of Model Error, Heights and Winds.

An empirical estimate was made of the autocorrelation function $\mu_{ij}$ by fitting a curve to correlations computed from actual data. The curve was taken to be of the form

$$\mu_{ij}(z) = (1 + \alpha|z_i - z_j|)\exp(-\alpha|z_i - z_j|)$$

where $Z_i$ is the ICAO height of level i. Some specimen curves of this type are shown in Fig A1. Values of $\alpha$ of 0.0003 (heights) and 0.0005 (winds) were regarded as giving the best approximation where $Z_i$ is measured in metres.

All of these statistics were derived as mean values appropriate to the T+12 hour forecast compared with the verifying analysed height or initialized wind field for an area lying between latitudes 35 deg and 65 deg N through the period 7th Sept., to 6th Oct. 1975.

Where the levels of observation do not coincide with the model levels it is necessary to interpolate between the data of Table 1 to provide appropriate values of model error; this was done using Lagrangian interpolation.

Horizontal Interpolation No attempt was made to allow for differences in geographical location in computing the variances, and accordingly for horizontal interpolation (33) may be expressed

$$\overline{(f_i - f_i^B)(f_j - f_j^B)} = \overline{(f_m - f_m^B)^2}\,\mu_{ij}(r) \qquad (34)$$

for level m, the model variance being drawn from Table 1 and the spatial correlation function assumed to be of the form

$$\mu_{ij}(r) = (1 + \beta r_{ij}) \exp(-\beta r_{ij})$$

as before, where $r_{ij}$ is the horizontal distance between the points i and j in grid-lengths, and $\beta$ has the value 0.78 for both heights and winds.

It will be noted that (34) is a drastically simplifying assumption: if the variance of the model error over the octagon is taken as constant isotropy and homogeneity are implied, and empirical estimation of F of equation (10) would in fact have been equally valid for purposes of the present experiment.

B. TREATMENT OF OBSERVATIONS AND OBSERVATIONAL ERROR

In the following paragraphs we look at the treatment of particular modes of observation, with particular reference to observational error.

(i) Height Data

Surface land observations: $\overline{\epsilon^2_{1000}} = 20\ m^2$

Surface ships: $\overline{\epsilon^2_{1000}} = 44\ m^2$

Upper Air land: Only the standard levels of radio-sonde TEMP reports were utilized. As with the GATE analysis, an assumption of constant temperature error throughout the sounding was made. Radio-sonde heights are derived from the measured temperature profile via the hydrostatic equation.
If $Z_i$ is the height of level i,

$$Z_i - Z_{1000} = -\int_{1000}^{P_i} \frac{R}{g} T \frac{dp}{p}$$

Accordingly

$$\epsilon_i - \epsilon_{1000} = -\int_{1000}^{P_i} \frac{R}{g} \epsilon_T \frac{dp}{p}$$

where $\epsilon_i$ is the error in height at level i, $\epsilon_T$ the temperature error through the sounding. Assuming $\epsilon_T$ to be constant

$$\epsilon_i = \epsilon_{1000} + \frac{R}{g}\epsilon_T \log_n \frac{1000}{P_i}$$

If we make the further assumption that $\epsilon_T$ and $\epsilon_{1000}$ are uncorrelated we may obtain an expression for the covariance of the height errors between levels:

$$\overline{\epsilon_i \epsilon_j} = \overline{\epsilon^2}_{1000} + \left(\frac{R}{g}\right)^2 \overline{\epsilon^2}_T \log_n \frac{1000}{P_i} \log_n \frac{1000}{P_j} \qquad (35)$$

and so

$$\overline{\epsilon^2}_{100} = \overline{\epsilon^2}_{1000} + \left(\frac{R}{g}\right)^2 \overline{\epsilon^2}_T \left[\log_n \left(\frac{1000}{100}\right)\right]^2$$

As $\overline{\epsilon^2}_{1000}$ is much smaller than $\overline{\epsilon^2}_{100}$ we may write

$$\overline{\epsilon^2}_{100} \simeq \left(\frac{R}{g}\right)^2 \overline{\epsilon^2}_T \left[\log_n \left(\frac{1000}{100}\right)\right]^2$$

and substitute for $\left(\frac{R}{g}\right)^2 \overline{\epsilon^2}_T$ in (35) to give

$$\overline{\epsilon_i \epsilon_j} = \overline{\epsilon^2}_{1000} + \overline{\epsilon^2}_{100} \cdot \frac{\log_n \frac{1000}{P_i} \log_n \frac{1000}{P_j}}{(\log_n 10)^2} \qquad (36)$$

from which an adequate estimate of the covariances may be obtained. For the present experiment $\overline{\epsilon^2}_{1000}$ was taken as $20m^2$, and $\overline{\epsilon^2}_{100}$ computed for each station in the appropriate Upper Air Station List using data available for the 12 months to December 1975. In the same processing estimates of the 100 mb sonde corrections were extracted for each station, to be applied prior to assimilation /9/.

It will be noted from (36) that

$$\overline{\epsilon_{1000} \epsilon_j} = \overline{\epsilon^2}_{1000}, \quad \text{for all } j \qquad (37)$$

This is to be expected: if we consider the terms contributing to $\overline{\epsilon_i \epsilon_j}$ we see it is composed of $\overline{\epsilon^2}_{1000}$ plus a term related to the error in thickness measured between 1000 mb and each of the levels i, j. If one of these levels is, in fact, 1000 mb, the error this contributes is zero.

Upper Air Ship: These reports were treated in the same way, taking

$$\overline{\epsilon^2}_{1000} = 44 \text{ m}^2$$

$$\overline{\epsilon^2}_{100} = 900 \text{ m}^2$$

SIRS Data

The error structure of SIRS was not well known, but was thought likely to be much in excess of the model error. Accordingly the observations were regarded as unsuitable for optimum interpolation in the vertical, and Lagrangian interpolation over the sounding used instead. A quadratic in $\log_n P$ was fitted in accordance with the following scheme:

| Level to be Interpolated. (mb) | Data Utilized (mb) |
|---|---|
| 600 | 500, 700, 850 |
| 800 | 700, 850, 1000 |
| 900 | 700, 850, 1000 |

The observational error is passed over to the subsequent horizontal interpolation. SIRS heights are reported relative to 1000 mb, so that it was necessary to utilize the forecast 1000 mb height as a datum. This leads to an overall error, for level p, of the form

$$\overline{\epsilon^2}_p = \overline{(h_{1000} - h^B_{1000})^2} + \overline{[\epsilon_p(\text{SIRS})]^2}$$

A suggested alternative is for the 1000 mb update to be carried out first in order to provide a better reference level. On such information as was available the SIRS errors were calculated to be:

| P (mb) | 100 | 200 | 300 | 400 | 500 | 600 | 700 | 800 | 900 | 1000 |
|---|---|---|---|---|---|---|---|---|---|---|
| $\overline{\epsilon_p(\text{SIRS})}^2_m$ | 5029 | 6022 | 4503 | 3114 | 1998 | 1267 | 746 | 392 | 132 | 0 |

Table A2: Variances of SIRS error

Recent work suggests that these figures may be too high, - certainly for present-day data, although they are smaller than those used for the GATE analysis. In any event, the upper levels can have received very little

weight in the optimum interpolation scheme. No attempt was made to allow for time differences: data within $\pm$ 1.5 hours of the assimilation time was utilized.

(ii) Wind Data

Surface land: Wind observations were not utilized as they are subject to too many disturbing influences (e.g. relief, coastal effects) to be considered representative of the 1000 mb contours.

Surface ship: $\overline{\epsilon^2}_{1000} = 4\ m^2 s^{-2}$ for both components. No allowance was made for the deviation of sea level pressure from 1000 mb; nor was this data used for interpolation to higher levels.

Upper Air, land and ship:

The GATE formula

$$\overline{\epsilon^2}_p = (4.9 - \alpha \log_{10} p)^2 \quad m^2 s^{-2} \qquad \text{(for level p)}$$

was used, $\alpha$ being allocated a value of 1.0. For purposes of optimum interpolation the errors were assumed to be random in the vertical. If less than three levels were reported no vertical interpolation was attempted.

Aircraft Reports: AIREPS were used only to extrapolate to the five upper model levels, the height of the observation commonly lying between 200 and 300 mb.

The error is of the form

$$\overline{\epsilon^2} = \overline{\epsilon^2}_{ob} + \overline{\sigma_t^2}\,\frac{\Delta t}{60}$$

for each component, where $\Delta t$ is the difference between observation time and analysis time in minutes, $\overline{\epsilon^2}_{ob}$ is an estimate of observational error, and $\overline{\sigma_t^2}$ an estimate of atmospheric variability. The values allocated were

$$\overline{\epsilon^2}_{ob} = (2.5)^2\ m^2 s^{-2}$$
$$\overline{\sigma_t^2} = (3.0)^2\ m^2 s^{-2}$$

GOES Winds: GOES data, the estimation of wind speeds by satellite measurement of cloud displacements, were not utilized in the present experiment, although the necessary programming was carried out.

(iii) Superobs Pairs of observations were combined to form superobs (Section 1.3) when they fell within 0.05 grid-lengths of each other. This was carried out at the data extraction stage for surface reports and, necessarily, after the filling of the block-directory for upper air data (Section 2.8). It will be remembered that an independent check of the sizes of the weights $q_i$ is also made at a late stage of the updating.

APPENDIX 2

ALTERNATIVE VERTICAL INTERPOLATION SCHEME

From equation (4)

$$f_l^I = f_l^B + \sum_{i=1}^{n} q_i (f_i^O - f_i^B)$$

This can be written

$$(f_l^I - f_l) = (f_l^B - f_l) + \sum_{i=1}^{n} q_i [(f_i^O - f_i) - (f_i^B - f_i)] \qquad (38)$$

or

$$\epsilon_l^I = \epsilon_l^B + \sum_{i=1}^{n} q_i (\epsilon_i^O - \epsilon_i^B)$$

Normally we minimise $\overline{\epsilon_l^{I\,2}} = \overline{(f_l^I - f_l)^2}$

We wish to interpolate to those model levels within a sounding where there are no observations and leave those levels which have observations as they are: i.e. we wish to obtain interpolated values consistent with the observed ascent. We also wish to obtain an estimate of the interpolation error.

Consider minimising the quantity

$$\overline{\varepsilon^2} = \overline{\left[(f_l^I - f_l) - \sum_{i=1}^{n} q_i (f_i^O - f_i)\right]^2}$$

i.e. the mean square of the difference between the interpolation error and the weighted sum of the errors of the observations, the weights being identical to those used in the interpolation of the new heights.

From (38)

$$\overline{\varepsilon^2} = \overline{\left[(f_l^B - f_l) - \sum_{i=1}^{n} q_i (f_i^B - f_i)\right]^2}$$

Setting $\frac{\partial \overline{\varepsilon^2}}{\partial q_i} = 0$ yields

$$\overline{\left[(f_l^B - f_l) - \sum_{j=1}^{n} q_j (f_j^B - f_j)\right](f_i^B - f_i)} = 0 \quad , \quad i = 1, 2, \ldots n$$

or

$$\sum_{j=1}^{n} q_j \overline{(f_j^B - f_j)(f_i^B - f_i)} = \overline{(f_l^B - f_l)(f_i^B - f_i)}, \quad i = 1, 2, \ldots n \qquad (39)$$

as the system of equations for the weights. This is analogous to (9) with an assumption of perfect observations. The interpolation error is from

$$E^2 = \overline{(f_1^I - f_1)^2} = \overline{\left[f_1^B - f_1 + \sum_{i=1}^{n} q_i (f_i^O - f_i^B)\right]^2}$$

(from 4)

$$\therefore E^2 = \overline{(f_1^B - f_1)^2} - 2\sum_{i=1}^{n} q_i \overline{(f_1^B - f_1)(f_i^B - f_i^O)} + \sum_i \sum_j q_i q_j \overline{(f_i^B - f_i^O)(f_j^B - f_j^O)}$$

If the observation errors are considered to be uncorrelated with the forecast errors, but possibly correlated amongst themselves we obtain

$$E^2 = \overline{(f_1^B - f_1)^2} - 2\sum_{i=1}^{n} q_i \overline{(f_1^B - f_1)(f_i^B - f_i)} + \sum_i \sum_j q_i q_j \left[\overline{(f_i^B - f_i)(f_j^B - f_j)} + \overline{\epsilon_i^O \epsilon_j^O}\right]$$

which from (39) becomes

$$E^2 = \overline{(f_1^B - f_1)^2} - \sum_{i=1}^{n} q_i \overline{(f_1^B - f_1)(f_i^B - f_i)} + \sum_i \sum_j q_i q_j \overline{\epsilon_i^O \epsilon_j^O}$$

Thus if 1 is an observation level, i, say

$$q_i = 1$$

$$q_j \ (i \neq j) = 0$$

and $$E^2 = \overline{\epsilon_i^{O\,2}}$$

and the observation is kept unchanged.

If the observation errors are random

$$E^2 = \overline{(f_1^B - f_1)^2} - \sum_i q_i \overline{(f_1^B - f_1)(f_i^B - f_i)} + \sum_{i=1}^{n} q_i^2 \overline{\epsilon_i^{O\,2}}$$

(c/f equation (12))

APPENDIX 3

ADJUSTMENT TO 1000 MB WIND FIELD FOLLOWING A HEIGHT UPDATE: TREATMENT OF FRICTION

For balanced flow we have

$$\frac{d\underset{\sim}{V}}{dt} = f\underset{\sim}{k}\times\underset{\sim}{V} + g\underset{\sim}{\nabla}h + g\frac{\partial\underset{\sim}{\tau}}{\partial p} = 0 \qquad (40)$$

If a rectangular coordinate system is used with the x axis aligned parallel to the contours

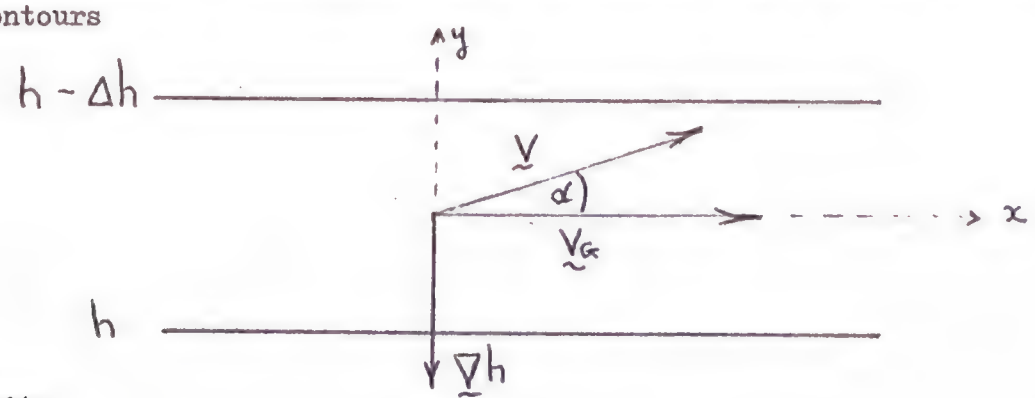


we may write

$$\frac{\partial h}{\partial y} = -\nabla h, \quad \frac{\partial h}{\partial x} = 0, \quad u = V\cos\alpha, \quad v = V\sin\alpha$$

where $\alpha$ is angle of cross-contour flow. Using

$\underset{\sim}{\tau} = \rho C_D V\underset{\sim}{V}$ (standard notation) and taking $\frac{\partial\underset{\sim}{\tau}}{\partial p}$ at 1000 mb to be $\frac{\underset{\sim}{\tau}}{\Delta p}$ where $\Delta p$ is 50 mb, (40) may be expressed

$$fv - g\frac{\partial h}{\partial x} - g\frac{\rho C_D V u}{\Delta p} = 0$$

$$-fu - g\frac{\partial h}{\partial y} - g\frac{\rho C_D V v}{\Delta p} = 0$$

Substituting for u, v, $\frac{\partial h}{\partial x}$, $\frac{\partial h}{\partial y}$ gives

$$\left.\begin{aligned} fV\sin\alpha - g\rho\frac{C_D V^2\cos\alpha}{\Delta p} &= 0 \\ -fV\cos\alpha + g\nabla h - g\rho\frac{C_D V^2\sin\alpha}{\Delta p} &= 0 \end{aligned}\right\} \qquad (41)$$

Solving for $\alpha$ and using the geostrophic relation we obtain

$$\sin\alpha = -\frac{\Delta p f}{2\rho g C_D V_G} + \sqrt{\left(\frac{\Delta p f}{2\rho g C_D V_G}\right)^2 + 1}$$

$$\cos\alpha = \sqrt{\frac{\Delta p f}{\rho g C_D V_G}\sin\alpha}$$

$$V = \sqrt{\frac{\Delta p f V_G}{\rho g C_D}\sin\alpha}$$

Substitution from these expressions into $u = V\cos\alpha$ , $v = V\sin\alpha$ gives

$$u = \frac{\Delta p f}{\rho g C_D}\left(-\frac{\Delta p f}{2\rho g C_D V_G} + \sqrt{\left(\frac{\Delta p f}{2\rho g C_D V_G}\right)^2 + 1}\right)$$

$$v = \sqrt{\frac{\Delta p f V_G}{\rho g C_D}}\left\{-\frac{\Delta p f}{2\rho g C_D V_G} + \sqrt{\left(\frac{\Delta p f}{2\rho g C_D V_G}\right)^2 + 1}\right\}^{3/2}$$

In order to convert to grid coordinates the transformation

$$u' = u\cos\psi - v\sin\psi$$
$$v' = u\sin\psi + v\cos\psi$$ is utilized,

where $\cos\psi = {}^{u_G}/_{V_G}$, $\sin\psi = {}^{v_G}/_{V_G}$ and $u_G$, $v_G$ are the components of $V_G$ in the grid coordinate system:

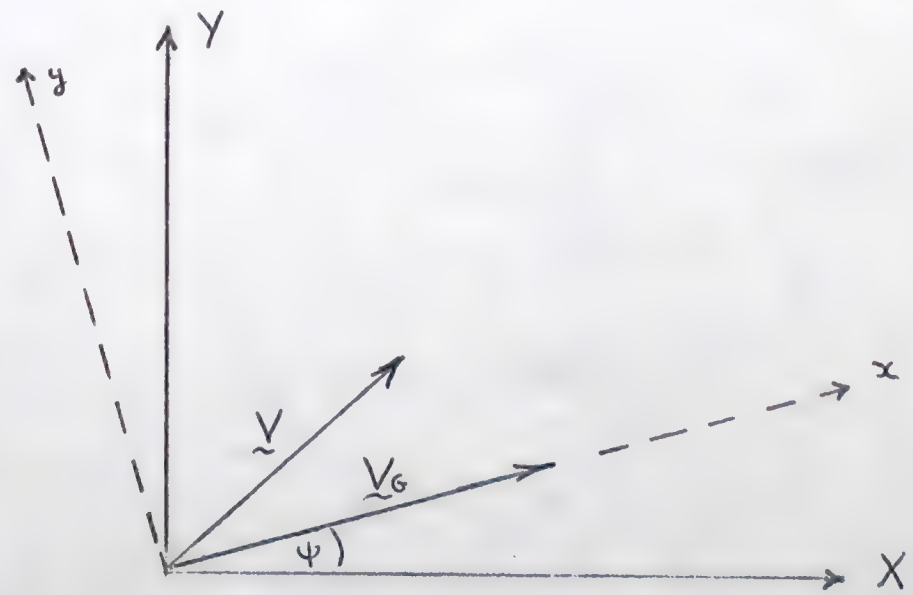

Thus finally

$$u' = u_G\left(\frac{\Delta p f}{\rho g C_D V_G}\right)\left(-\frac{\Delta p f}{2\rho g C_D V_G} + \sqrt{\left(\frac{\Delta p f}{2\rho g C_D V_G}\right)^2 + 1}\right)$$

$$- v_G\left(\frac{\Delta p f}{\rho g C_D V_G}\right)^{1/2}\left(-\frac{\Delta p f}{2\rho g C_D V_G} + \sqrt{\left(\frac{\Delta p f}{2\rho g C_D V_G}\right)^2 + 1}\right)^{3/2}$$

$$v' = v_G\left(\frac{\Delta p f}{\rho g C_D V_G}\right)\left(-\frac{\Delta p f}{2\rho g C_D V_G} + \sqrt{\left(\frac{\Delta p f}{2\rho g C_D V_G}\right)^2 + 1}\right)$$

$$+ u_G\left(\frac{\Delta p f}{\rho g C_D V_G}\right)^{1/2}\left(-\frac{\Delta p f}{2\rho g C_D V_G} + \sqrt{\left(\frac{\Delta p f}{2\rho g C_D V_G}\right)^2 + 1}\right)^{3/2}$$

---

APPENDIX 4

ALTERNATIVE METHODS OF MODIFYING THE DIVERGENCE FIELD AFTER A WIND UPDATE

The Washington and Baumhefner method modifies the updated divergence field so that the vertically averaged divergence over any column of the model is approximately zero.

We calculate the updated divergence

$$D_u = \frac{\partial v_u}{\partial y} + \frac{\partial u_u}{\partial x}$$

as before, and also the field

$$\overline{D_u} = -\int_{1000}^{100} D_u \, dp \Big/ 900,$$

the average divergence over each model column.

Introduce a mean velocity potential $\bar{\phi}$ such that

$$\nabla^2 \bar{\phi} = \overline{D_u}$$

and solve this equation subject to boundary conditions

$$\frac{\partial \bar{\phi}}{\partial n} = 0$$

On solution, increment the updated velocity field at all levels by

$$\delta u = -\frac{\partial \bar{\phi}}{\partial x}, \quad \delta v = -\frac{\partial \bar{\phi}}{\partial y}$$

The result is a new divergence field

$$D = D_u - \overline{D_u}, \quad \text{for which } \bar{D} = 0$$

A variation on this modifies the updated divergence field so that the vertically averaged divergence over any column of the model is restored to that holding before the update. We replace $D_u$ by the difference between the forecast and updated divergence. The other steps are much the same as before, and the result is a new divergence field

$$D = D_u - (\overline{D_u} - D_F)$$

for which $\bar{D} = \bar{D}_F$

Surface Pressure

Isobars at 4 mb intervals

Fig 3.1 Operational main-run analysis at ØØZ, 30/12/75

Surface Pressure

Isobars at 4 mb intervals

Fig 3.2 12 hour operational forecast to 12Z, 30/12/75

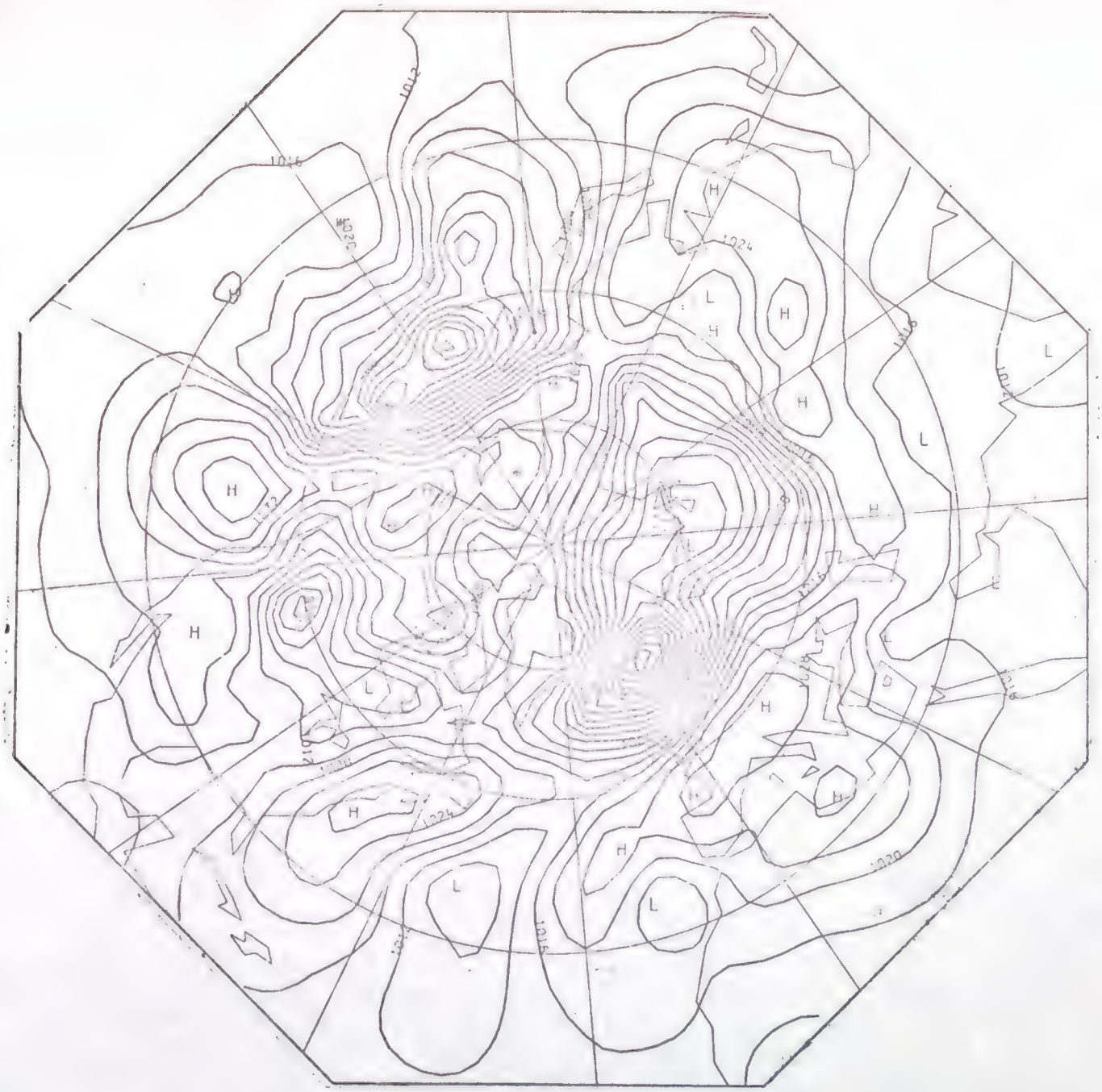


Fig 3.3 Operational update analysis at 12Z, 30/12/75

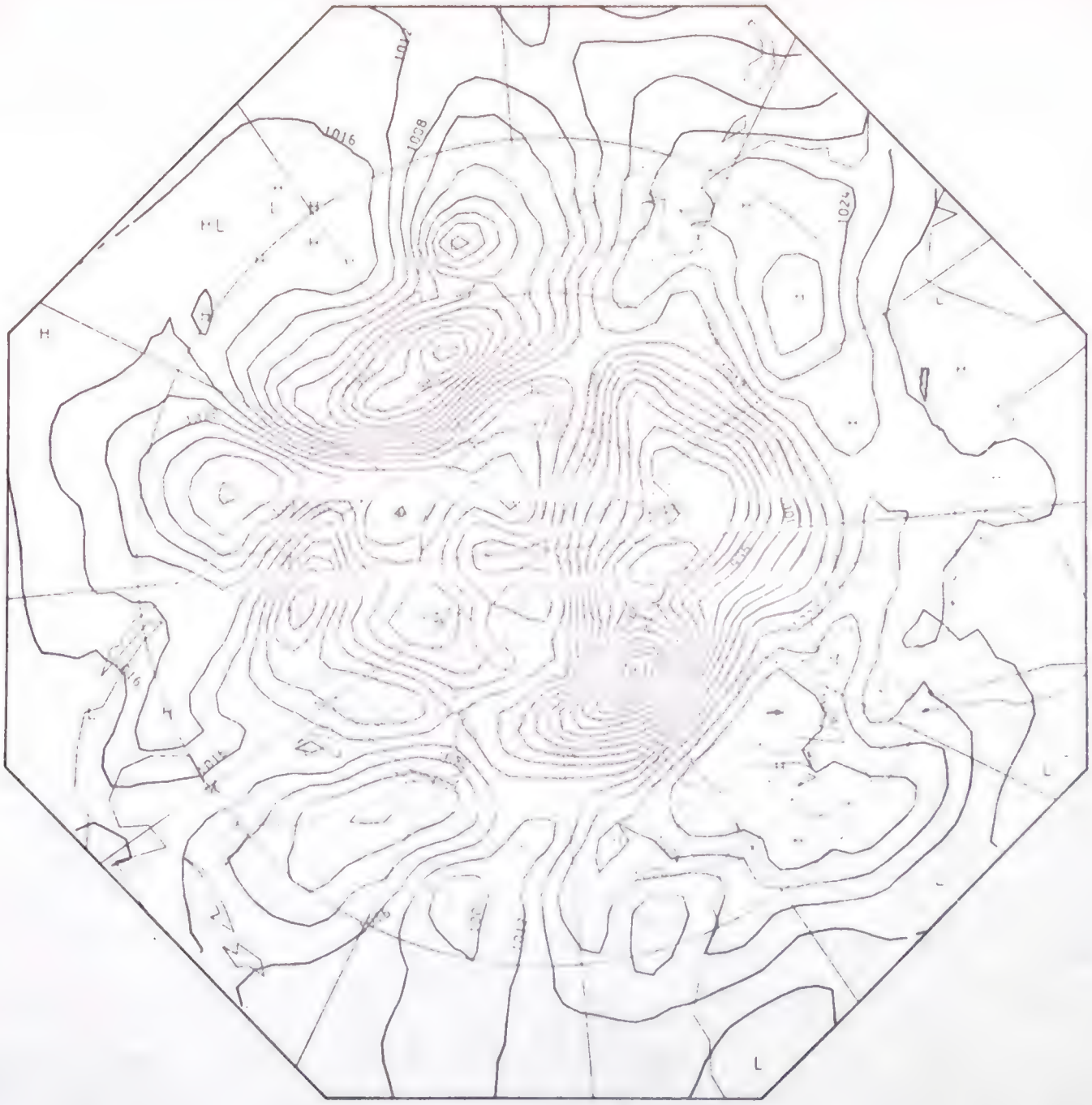


Surface Pressure

Isobars at 4 mb intervals

Fig 3.4 12 hour heights-assimilated forecast to 12Z, 30/12/75

Surface Pressure

Isobars at 4 mb intervals

Fig 3.5 12 hour winds-assimilated forecast to 12Z, 30/12/75

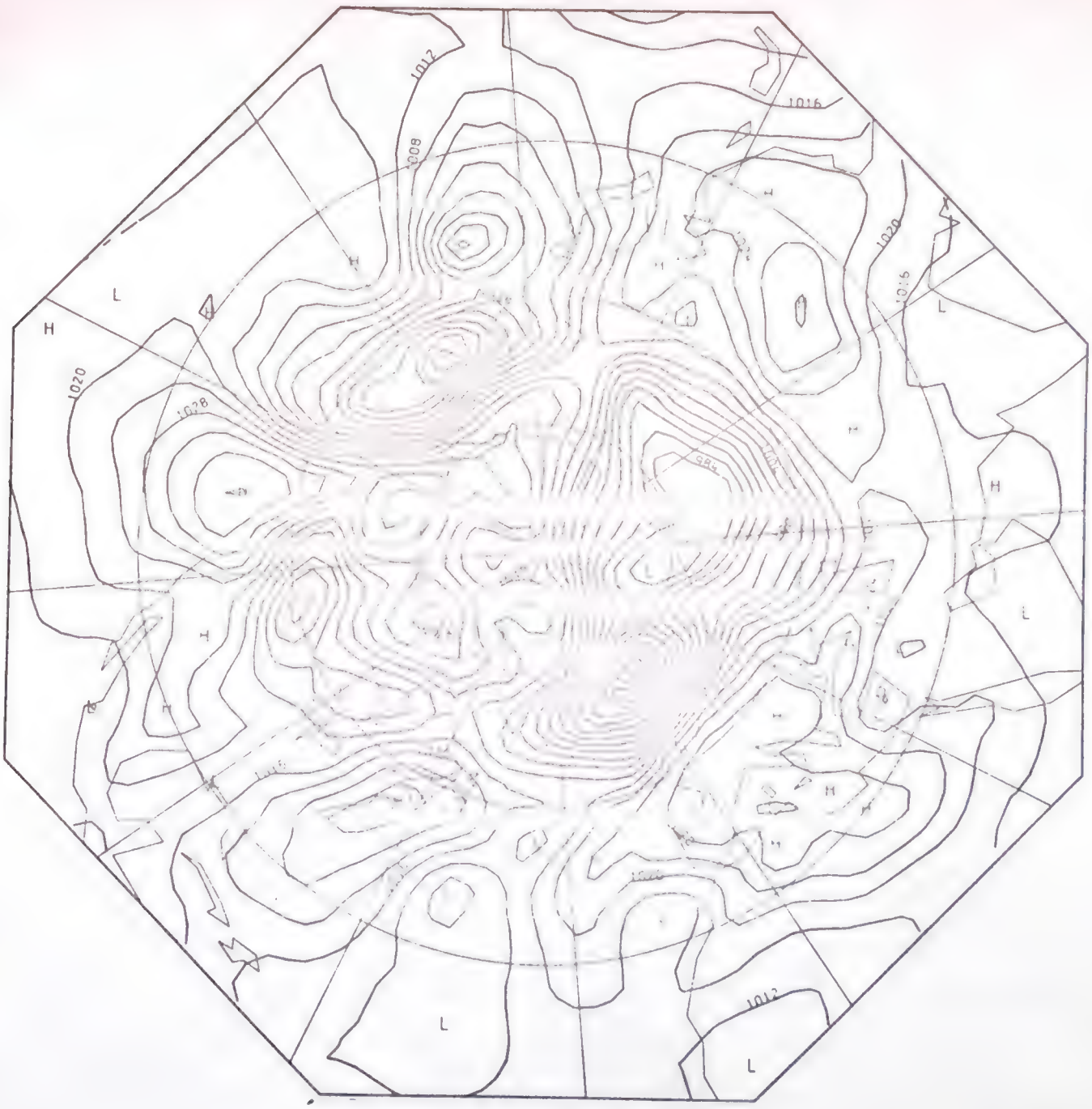


Surface Pressure

Isobars at 4 mb intervals

Fig 3.6 12 hour heights+winds-assimilated forecast to 12Z, 30/12/75

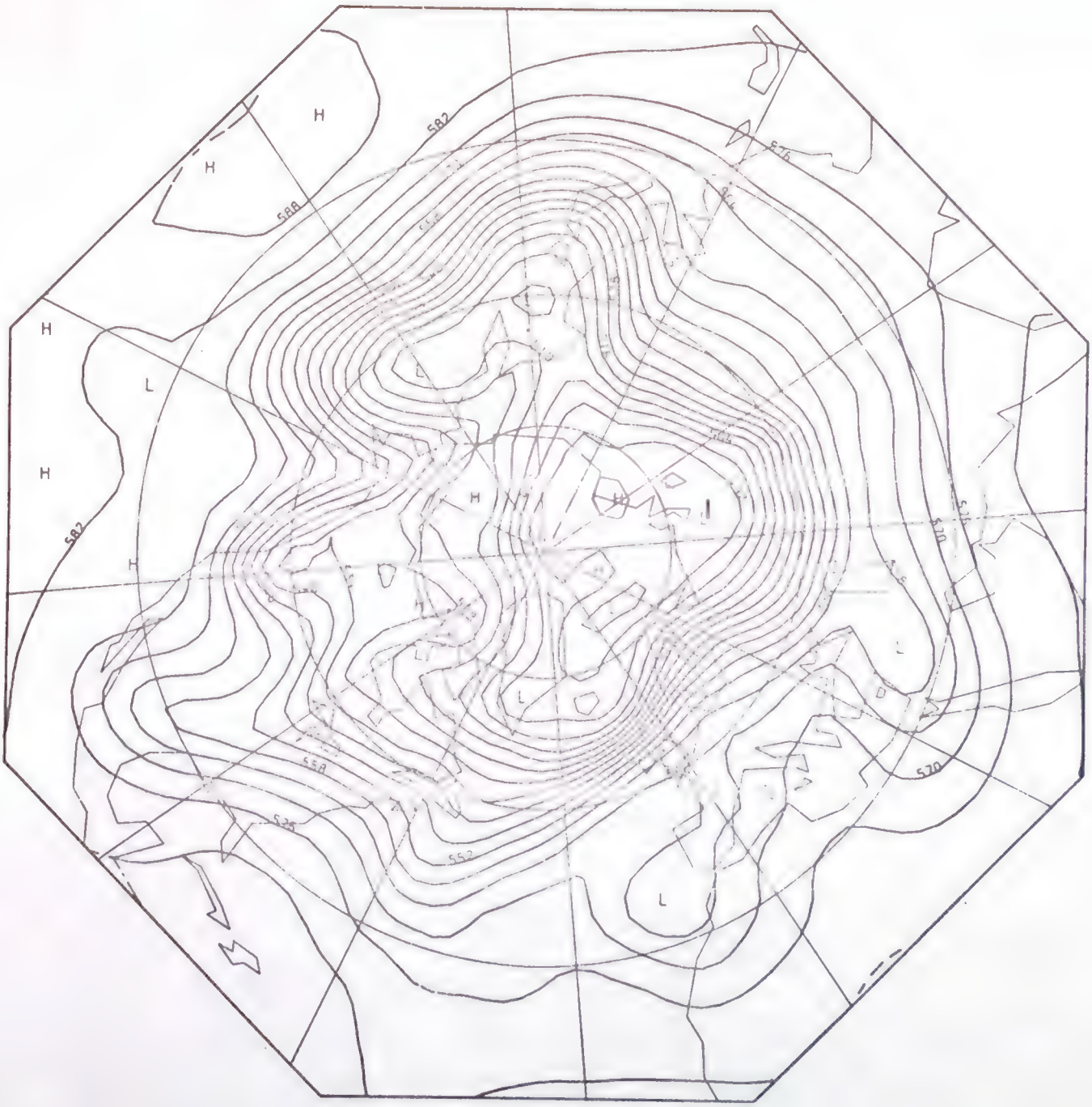


500 mb contours

Contour lines at 6 dm intervals

Fig 3.7 12 hour operational forecast to 12Z, 30/12/75

H
L
H
L
H
H
L
H
L
H
H
H
H
L
L
H
H
L
H
H
H
H

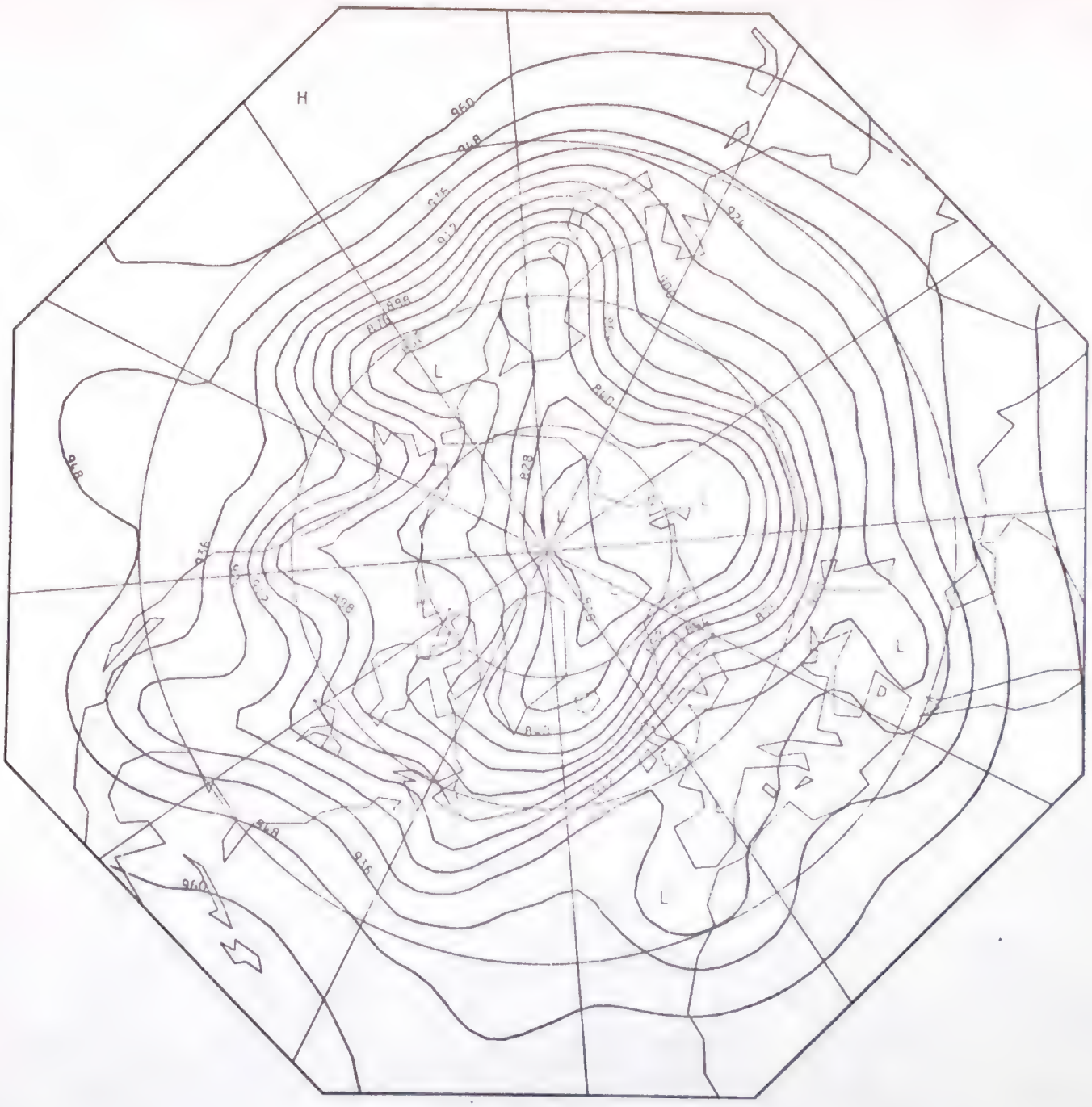
H
960
948
936
924
912
900
888
876
864
852
840
828
816
804
792
780
768
756
744
732
720
708
696
684
672
660
648
636
624
612
600
588
576
564
552
540
528
516
504
492
480
468
456
444
432
420
408
396
384
372
360
348
336
324
312
300
288
276
264
252
240
228
216
204
192
180
168
156
144
132
120
108
96
84
72
60
48
36
24
12
0
L
L
L

300 mb contours

Contour lines at 12 dm intervals

Fig 3.10 12 hour heights+winds assimilated forecast to 12Z, 30/12/75

Fig 3.11

ASSIMILATED FORECASTS TO
12 Z, 30/12/75.

RMS ERROR OVER OCTAGON, (HEIGHTS)

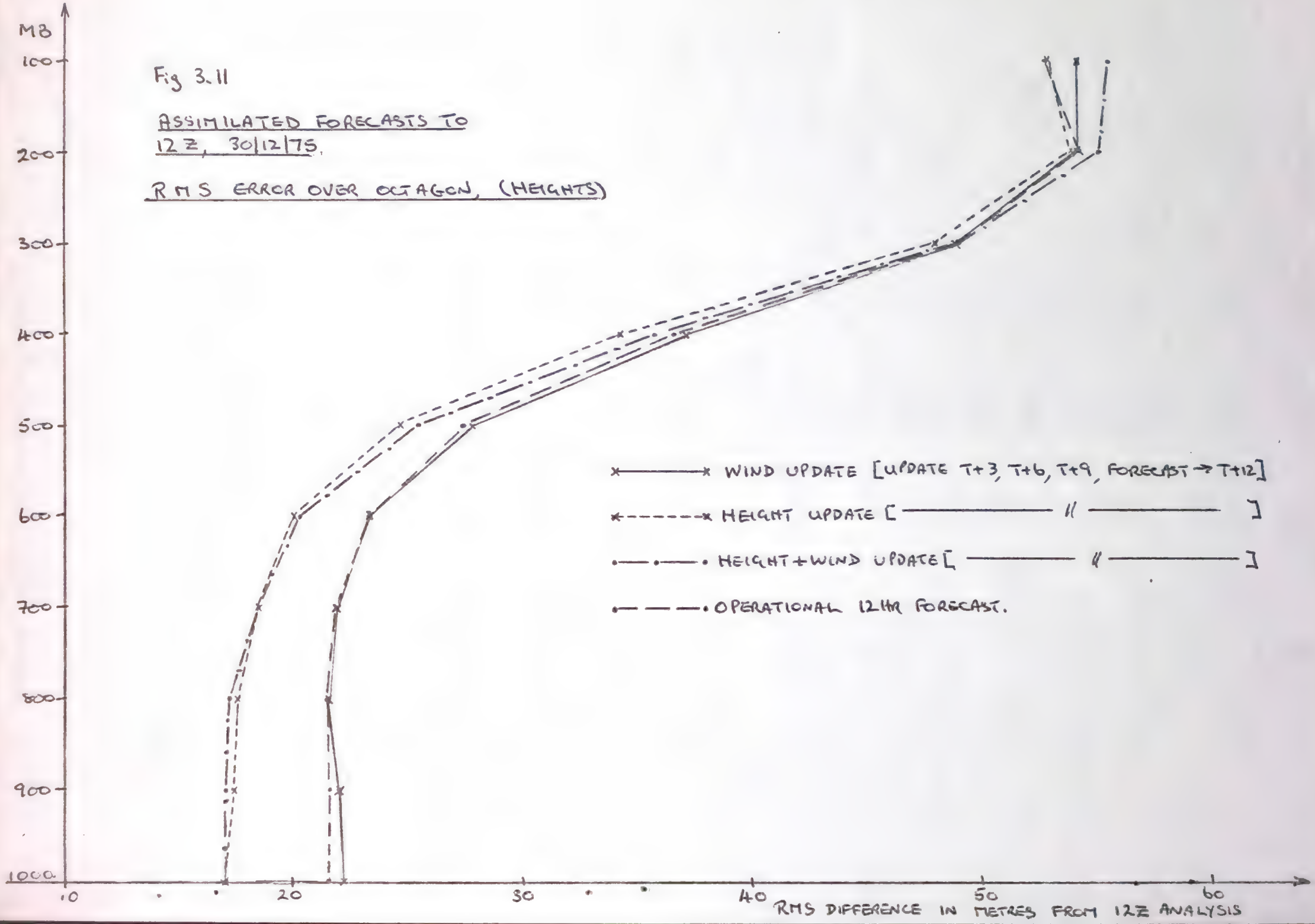

Surface Pressure Isobars at 4 mb intervals

Fig 3.12 Operational main-run analysis at 12Z, 30/12/75

Fig 3.13 Analysis at 12Z, 30/12/75 based upon heights+winds assimilated forecast.

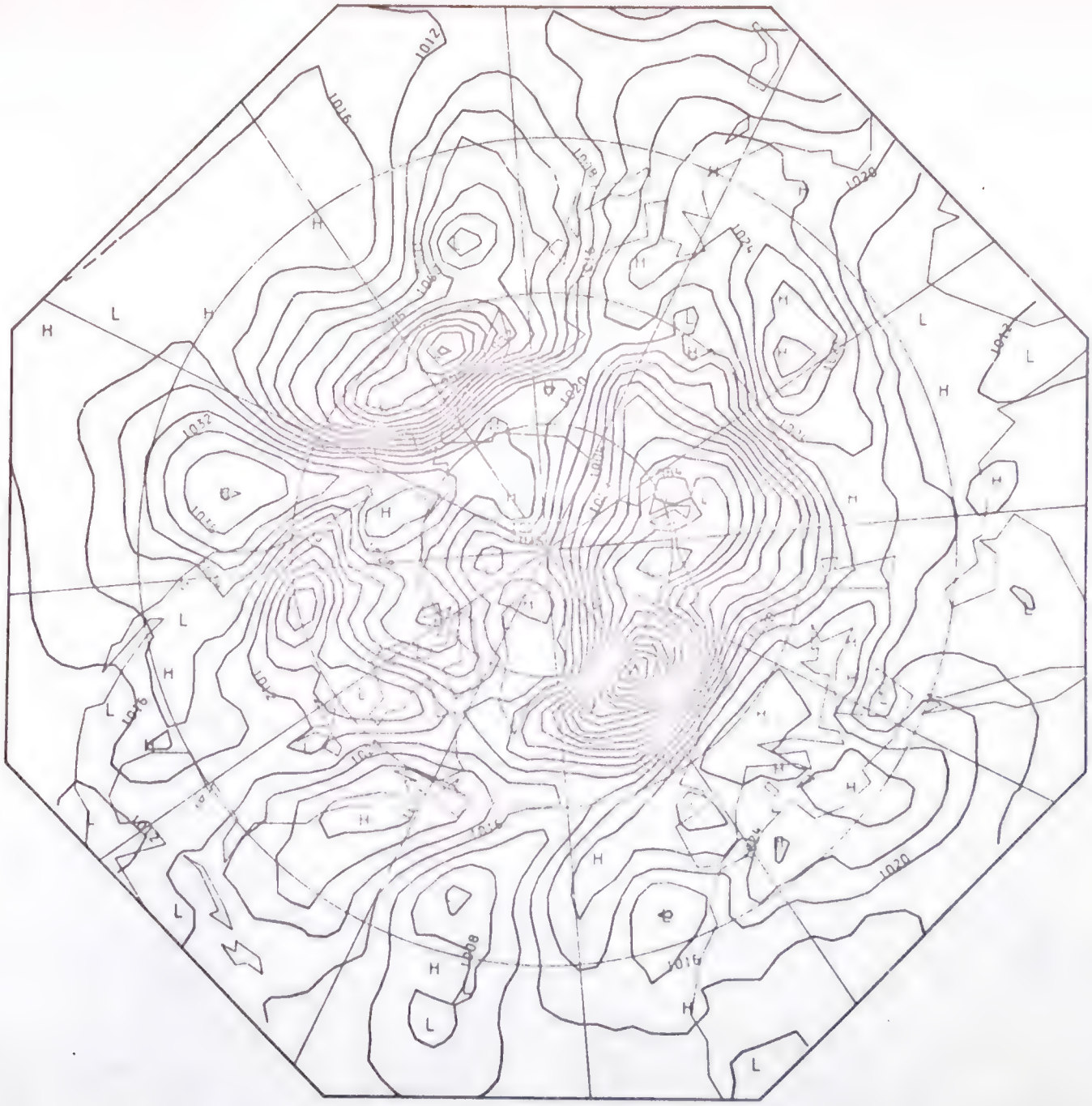


Surface Pressure

Isobars at 4 mb intervals

Fig 3.14 Heights+winds update, 12Z, 30/12/75

Surface Pressure

Isobars at 4 mb intervals

Fig 3.15 12 hour forecast to ØØZ, 31/12/75 from 12Z operational main-run analysis

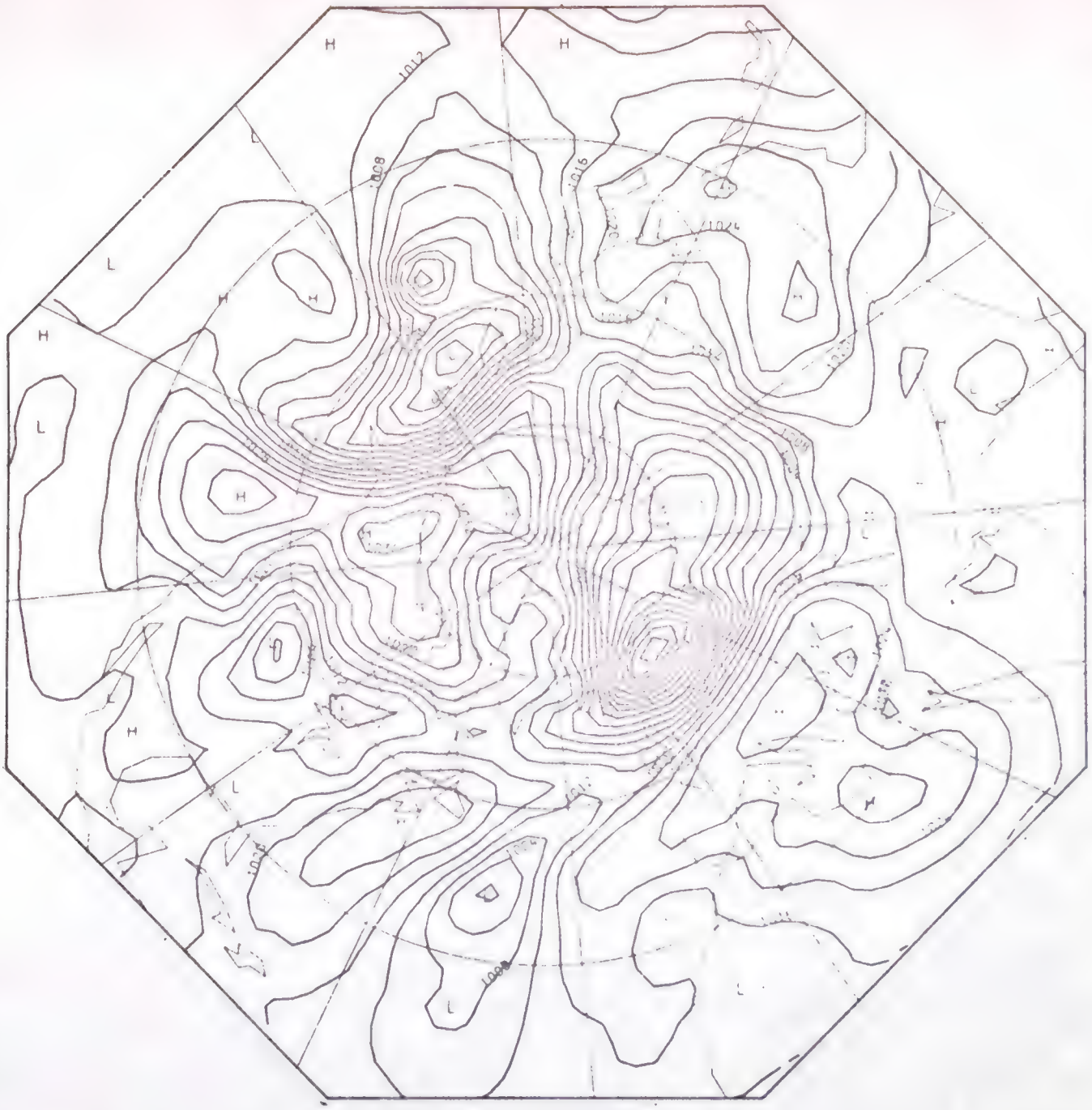


Surface Pressure

Isobars at 4 mb intervals

Fig 3.16 12 hour forecast to ØØZ, 31/12/75 from 12Z heights+winds update.

Fig 3.17

12 HR FORECASTS TO ϕϕZ, 31|12|75

FROM T+12 INITIALIZATIONS, ETC.

RMS ERROR OVER OCTAGON, (HEIGHTS)

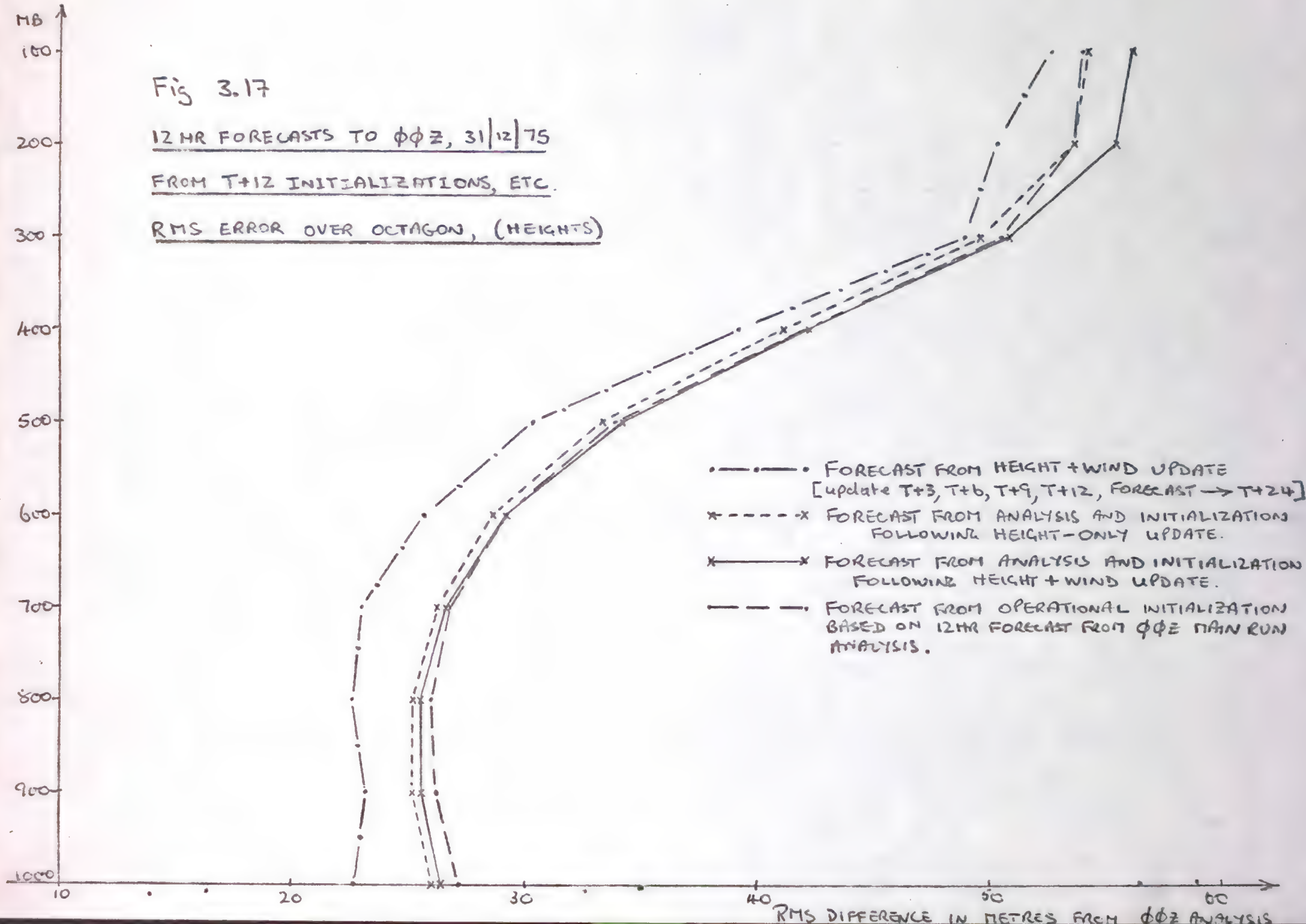

Fig 4.1

EFFECT OF VARIOUS METHODS OF DAMPING UNWANTED OSCILLATIONS FOLLOWING A TRIAL WIND UPDATE (ASSIMILATING AIREPS AND SURFACE SHIP WINDS)

(FROM UNPUBLISHED WORK BY DICKINSON)

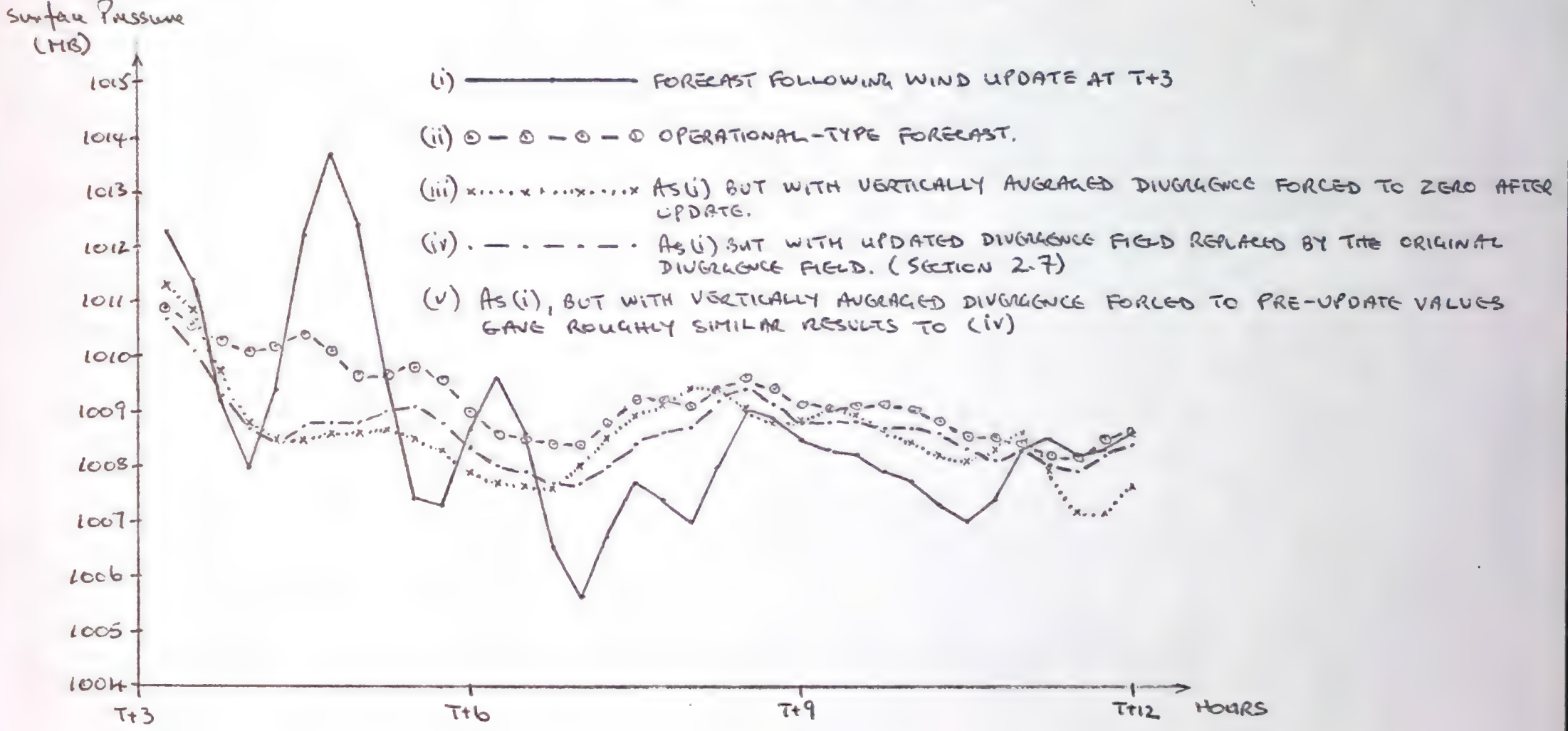

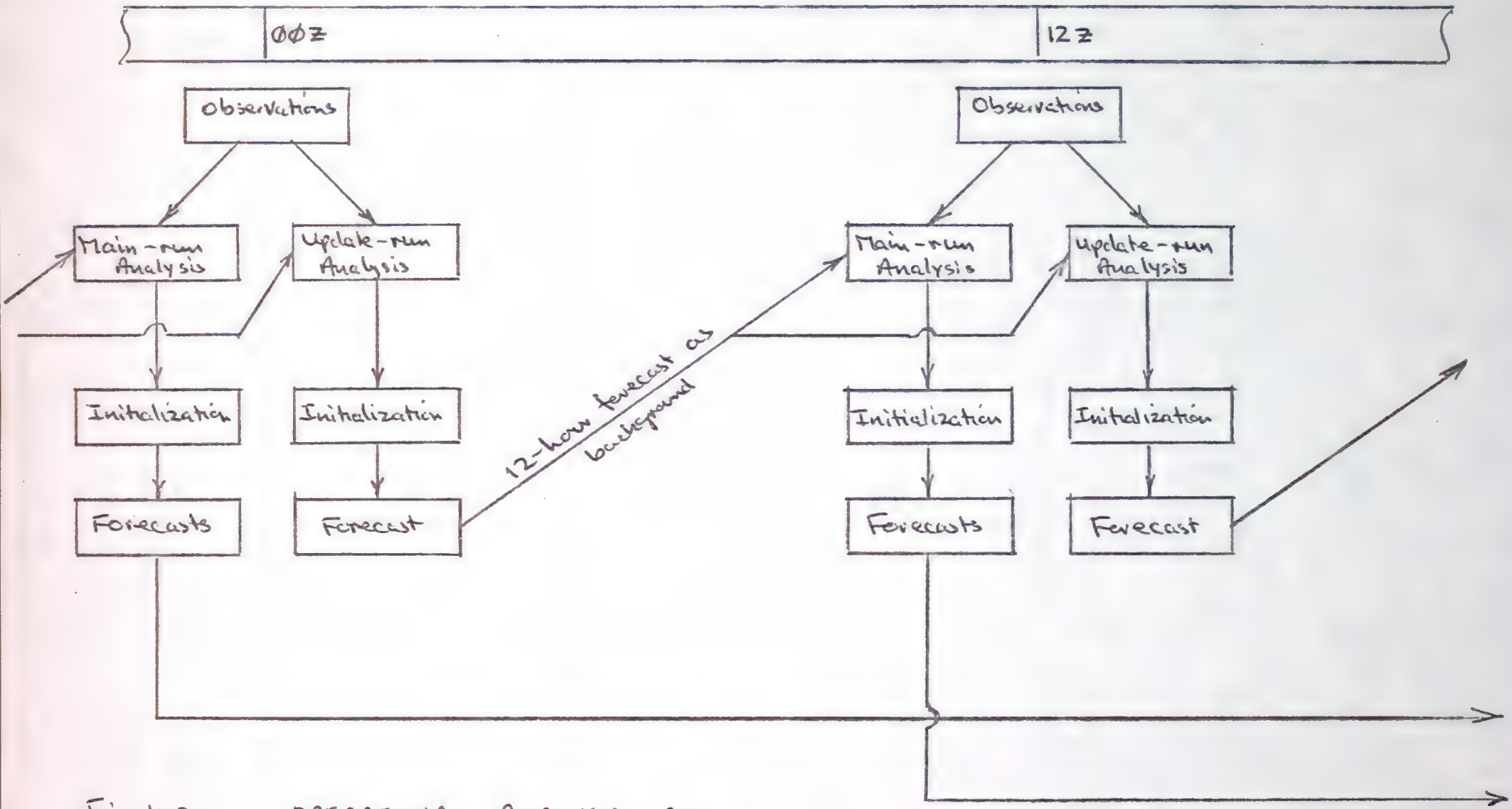


Fig 4.2 OPERATIONAL ANALYSIS AND FORECAST CYCLE.

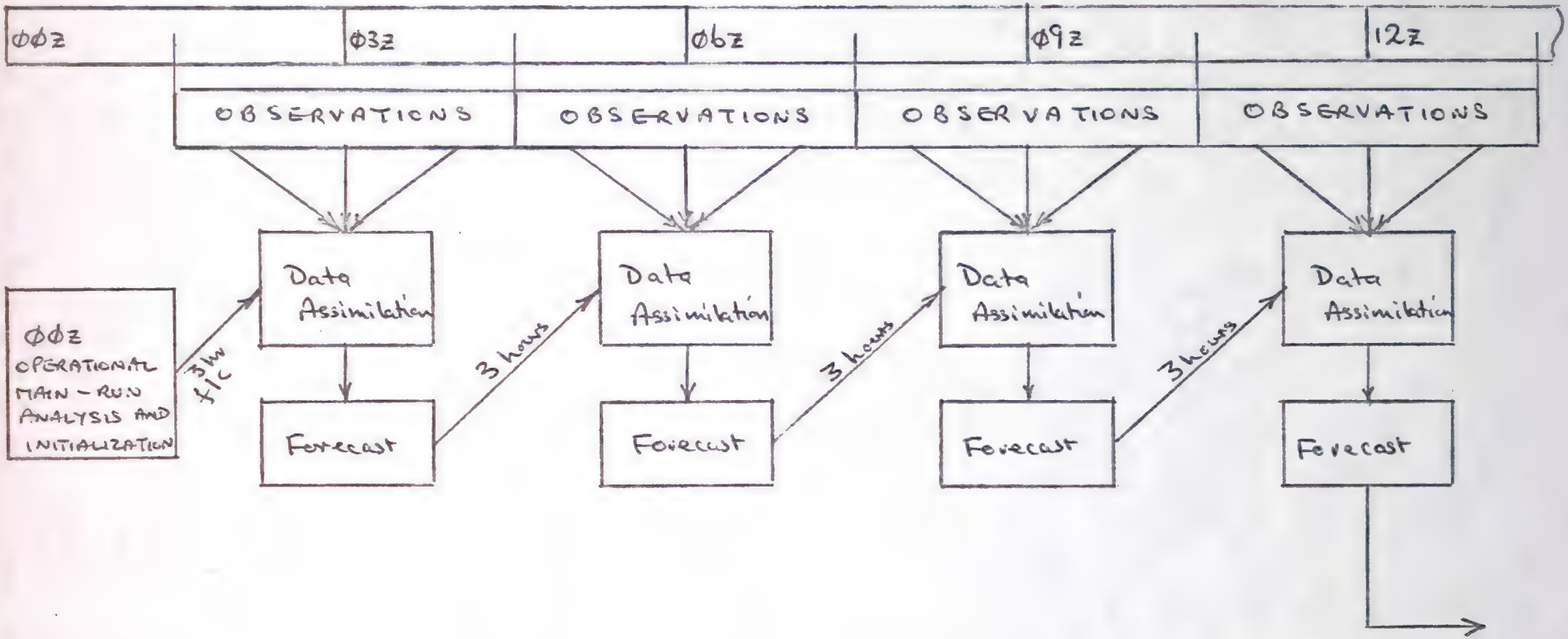


Fig 4.3 MET O 11 PILOT EXPERIMENT: INTERMITTENT DATA ASSIMILATION

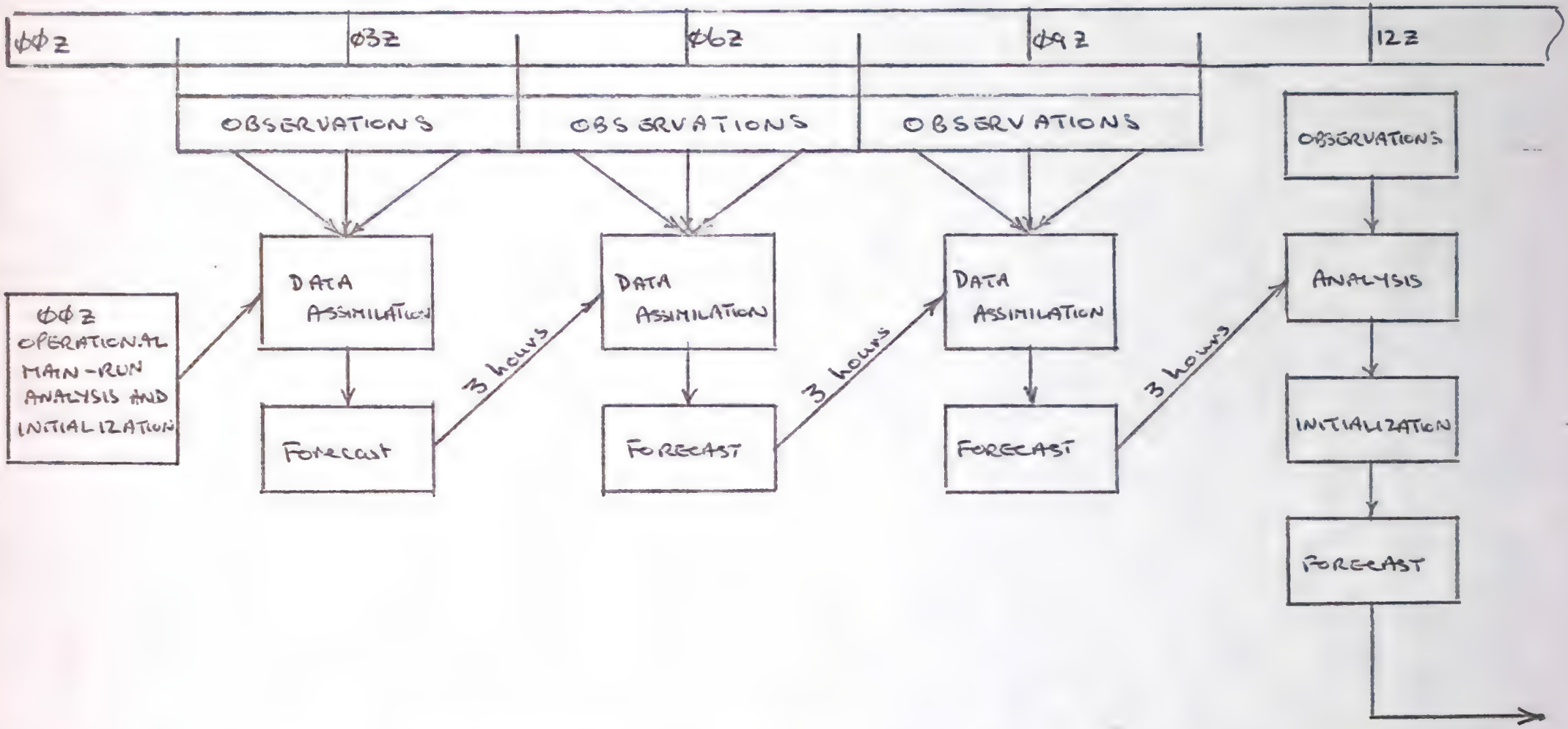


Fig 4.4 — METEOSAT PILOT EXPERIMENT: PROVISION OF AN IMPROVED BACKGROUND FIELD

Fig A.1 SPECIMEN CURVES OF THE FORM $\mu(x) = (1+\alpha x)e^{-\alpha x}$

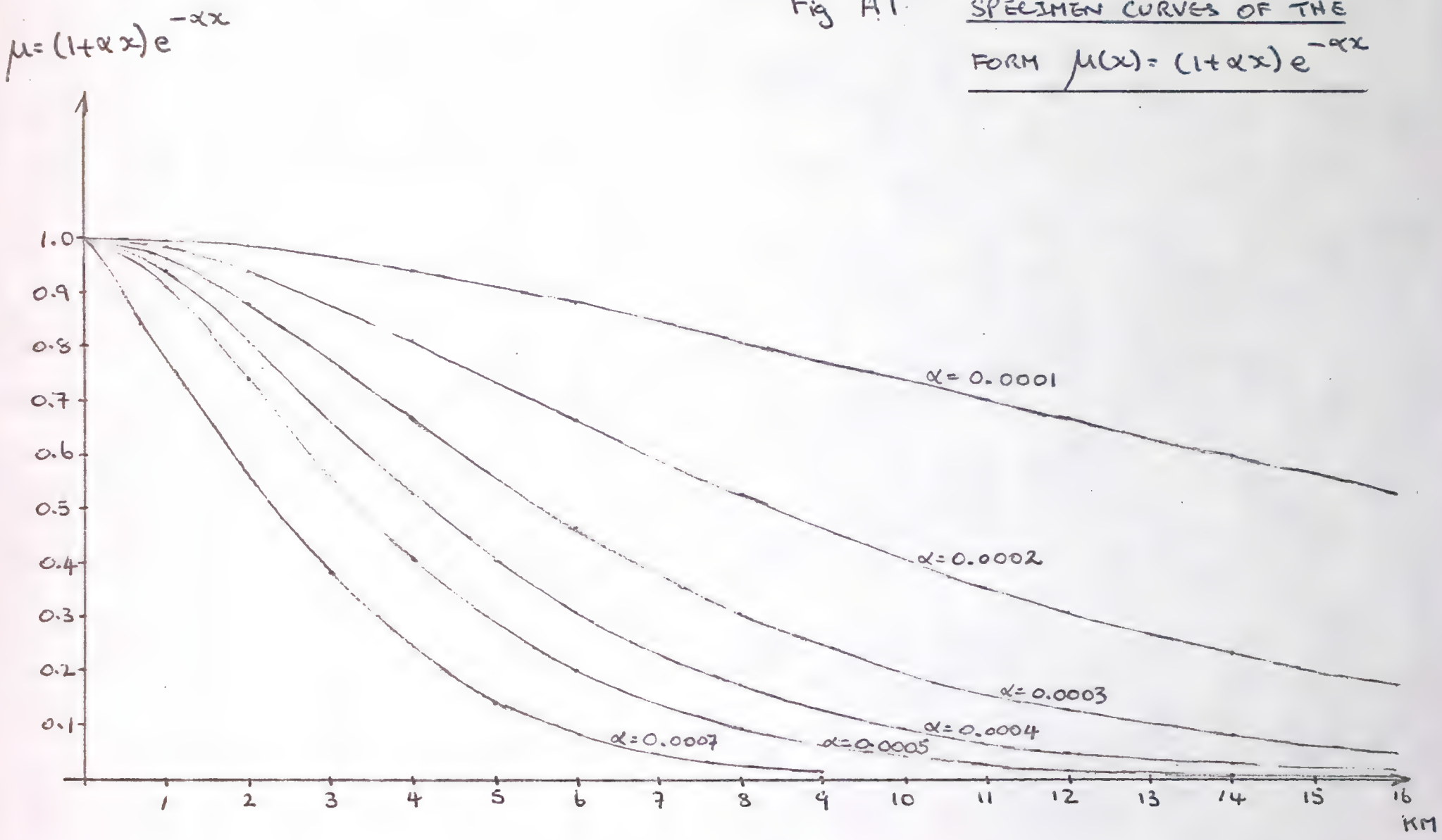

SUPPLEMENT

## THE EXPERIMENT OF 29th MARCH 1977

Opportunity is taken to append brief details of a second experiment which was in progress while this paper was in preparation. The approach was similar to that used previously, with attention confined to a straight combined height+wind assimilation run. The 12Z operational update-run analysis of 29th March 1977 was taken as a starting point, and data assimilation carried out up to and including ØØZ on 30th. This, without conventional initialization, formed a basis for a 12 hour forecast. For purposes of comparison a 12-hour operational forecast from the same start dataset was used as a background for the usual analysis and initialization at ØØZ, and a further 12-hour forecast made.

### Model and Observational Error

The availability of more recent computations of forecast error led to a reappraisal of the model error variances used for the optimum interpolation. The following figures were adopted:

| P(mb) | 100 | 150 | 200 | 250 | 300 | 400 | 500 | 600 | 700 | 800 | 850 | 900 | 1000 |
|---|---|---|---|---|---|---|---|---|---|---|---|---|---|
| $(h-h_B)^2 m^2$ | 1300 | 1380 | 1420 | 1360 | 1275 | 830 | 575 | 460 | 400 | 360 | 360 | 365 | 380 |
| $(u-u_B)^2$, $(v-v_B)^2$ $(m/s)^2$ | 18.5 | 25.0 | 28.5 | 31.5 | 33.0 | 23.0 | 17.0 | 14.0 | 11.5 | 10.5 | 10.0 | 9.5 | 10.0 |

New values were also substituted for some observational errors following perusal of more recent estimates, which were obtained from Met O 2:

AIREPS: $\overline{\epsilon^2_{ob}} = (6.0)^2 \, m^2 s^{-2}$

SIRS:

| P(mb) | 100 | 200 | 300 | 400 | 500 | 600 | 700 | 800 | 900 | 1000 datum |
|---|---|---|---|---|---|---|---|---|---|---|
| $\sum_{m^2} p^{(SIRS)^2}$ | 2900 | 2800 | 2200 | 1600 | 1100 | 700 | 400 | 250 | 100 | 0 |

GOES winds were utilized in this experiment. The observations and errors were treated in a similar manner to AIREPS. Extrapolation was carried out from the reporting level to the 5 uppermost model levels; for lower tropospheric data, however, assimilation was confined to the attributed level of 900 mb together with an extrapolation to 1000 mb. The error estimates were based on a recent comparison of GOES reports with verifying analyses:

$\overline{\epsilon^2_{ob}} = (4.5)^2 m^2 s^{-2}$ for the lower troposphere

$\overline{\epsilon^2_{ob}} = (8.0)^2 m^2 s^{-2}$ for the upper troposphere

The timely publication of a Met O 20 Technical Note /15/ on the performance of radio-sondes through 1976 enabled a fresh list of sonde 100 mb error variances to be prepared. When the new list was compiled the variances were limited to an arbitrary maximum of 2500 $m^2$. At the same time the operational sonde 100 mb error corrections were substituted for the old specially computed values, as it was thought this might provide a better comparison with the results of the operational-type procedures.

Quality Control

The test of fresh reports against adjacent observations (equations (24), (25)) was made less stringent for winds, the new formulation being

$$|u^c - u^o| > 4\sqrt{\epsilon^2_o + \epsilon^2_c}$$

Computation by Gandin et al, /1/ suggests that a coefficient of 4 gives the most satisfactory result, and this is in accordance with such study as was made of the effects of the quality control during the earlier experiment.

Preliminary Results

As before, and as is to be expected, the assimilated forecast up to T+12 (ØØZ 30th March) was superior to the 12-hour operational forecast. Comparisons with the Central Forecasting Office plotted charts also confirmed that the analysis provided by the height+wind assimilation at T+12 gave better results than the operational product for that time. The 12-hour forecasts (to 12Z 30th March) run from the two analyses, however, did not, on comparison, yield clearcut results. A depression in the Central North Atlantic deepened very rapidly during this forecast period, and neither forecast coped with it at all well. The forecast from the assimilation was slightly superior in this respect, but other synoptic features were handled better by the forecast from the conventional initialization. The results on the whole were not very conclusive.

A graphical comparison of the root mean square of height error of the forecasts (using an operational update analysis as verification) is given in fig S.1. The forecast from the assimilation does not compare very well with the operational product. This runs contrary to the results of the corresponding test for the earlier experiment. As before, however, there is a possibility of some bias in favour of the conventional run.

In an attempt to explain this apparently poor performance the question of the generation of gravity waves is being investigated. Fig S.2 shows the variation in a spot value of surface pressure during the forecast following the height+wind assimilation at T+12. Considerable oscillation is taking place in spite of the divergence adjustment. It is beginning to look as if the assimilation of large quantities of data at the main (and perhaps some intermediate) synoptic hours may present larger problems than can be dealt with by means of the divergence adjustment alone.

Recent work has been directed towards investigating the effects of employing some other techniques for damping spurious waves. Figs S.1 and S.2 are also used to show the results of (a) subjecting the T+12 height+wind assimilation to a 20 timestep (5 hour) dynamic initialization prior to the forecast, and (b) using a damped integration scheme for the forecast. Details of these techniques will be found in "An Implicit Dynamic Initialization Scheme" by Miss M J Atkins.

It is apparent that either of these refinements improve the RMS to a point where favourable comparisons with the operational run are obtained, although the situation at 1000 mb is disappointing. The damped integration is particularly effective in removing undesirable oscillations and reducing the RMS height error. We may reasonably infer that the poor performance of the forecast from the midnight update was indeed the result of spurious waves rather than any shortcoming in the analysis provided by the assimilation, although some scrutiny of the data assimilated at 1000 mb may be called for.

Fig S.3 illustrates the effects of applying the same damping procedures to the forecast of Fig 4.1. This was a case for which no divergence modification had been attempted. The results appear to be very satisfactory, and some future investigation could perhaps be turned towards combining 4-dimensional data assimilation (pruned of its divergence adjustment) with a damped integration scheme as being the combination most likely to give good results at a reasonable computational cost.

Fig S.i: RMS HEIGHT ERROR OVER OCTAGON:

12 HR FORECASTS TO 12Z 30/3/77

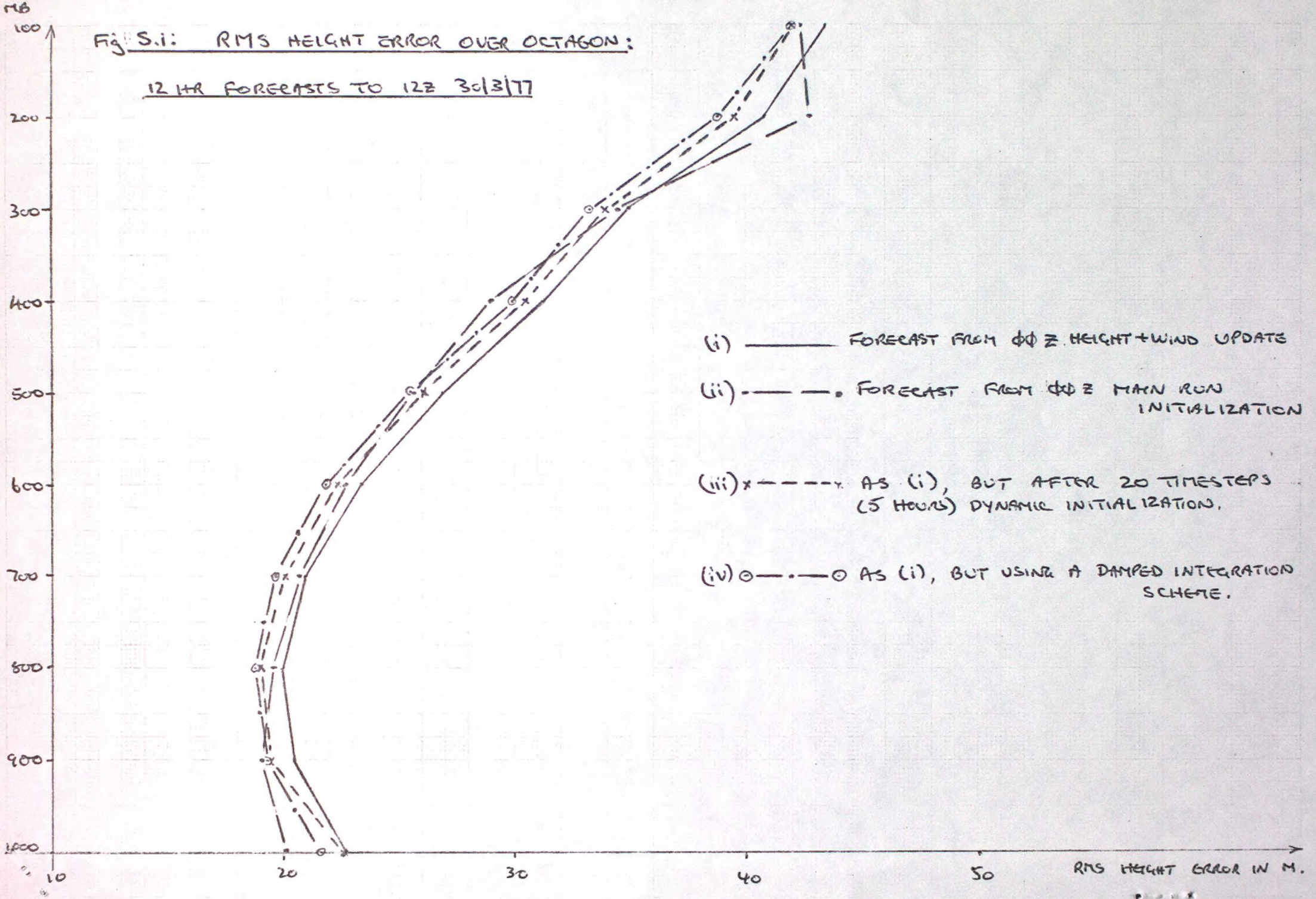

Fig. S.2: EFFECT OF DYNAMIC INITIALIZATION AND DAMPED INTEGRATION ON THE FORECAST FROM THE HEIGHT+WIND UPDATE, ΦΦZ, 3C|3|77.

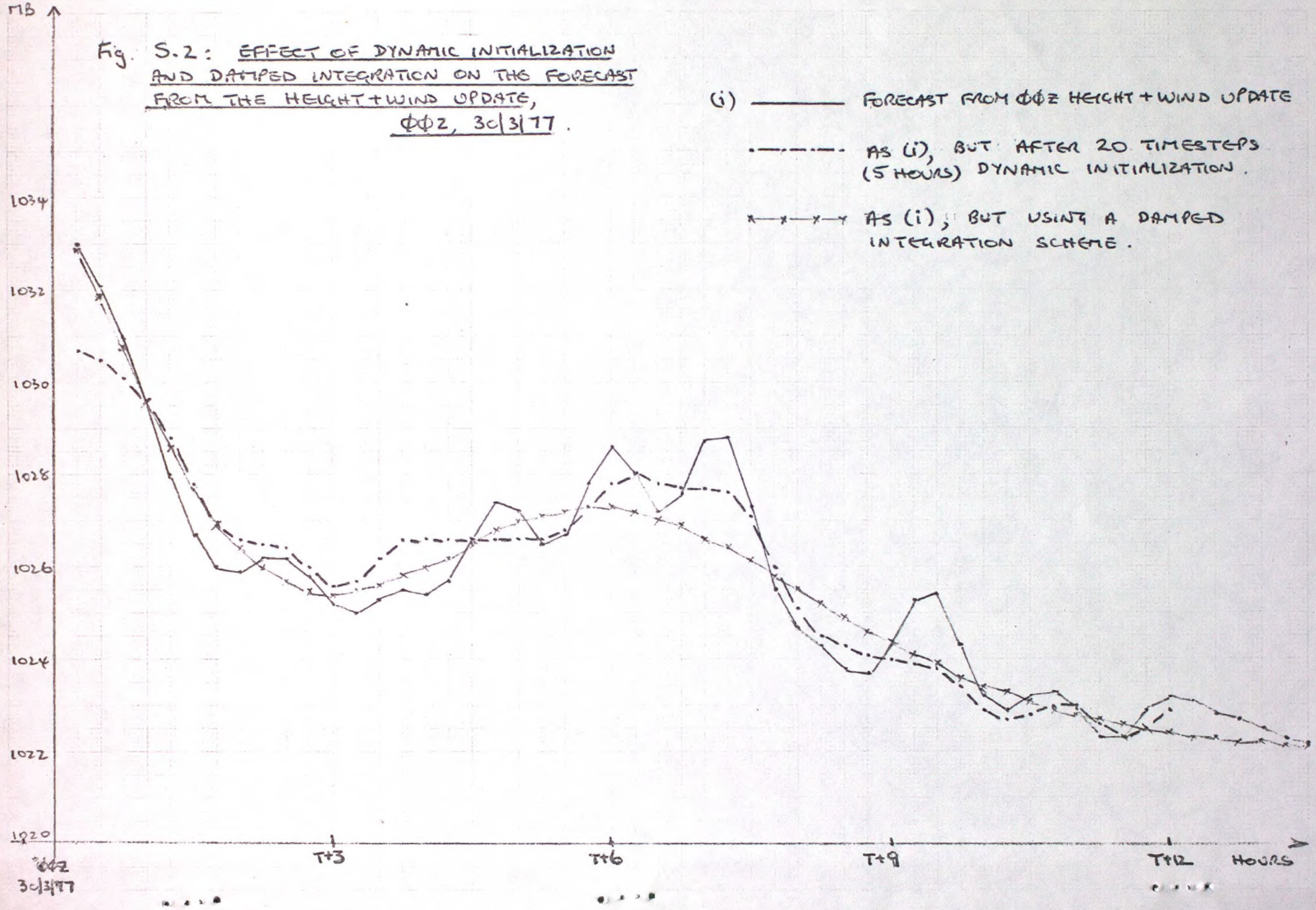


(i) ——— FORECAST FROM ΦΦZ HEIGHT+WIND UPDATE

·—·—·—· AS (i), BUT AFTER 20 TIMESTEPS (5 HOURS) DYNAMIC INITIALIZATION.

×—×—×—× AS (i); BUT USING A DAMPED INTEGRATION SCHEME.
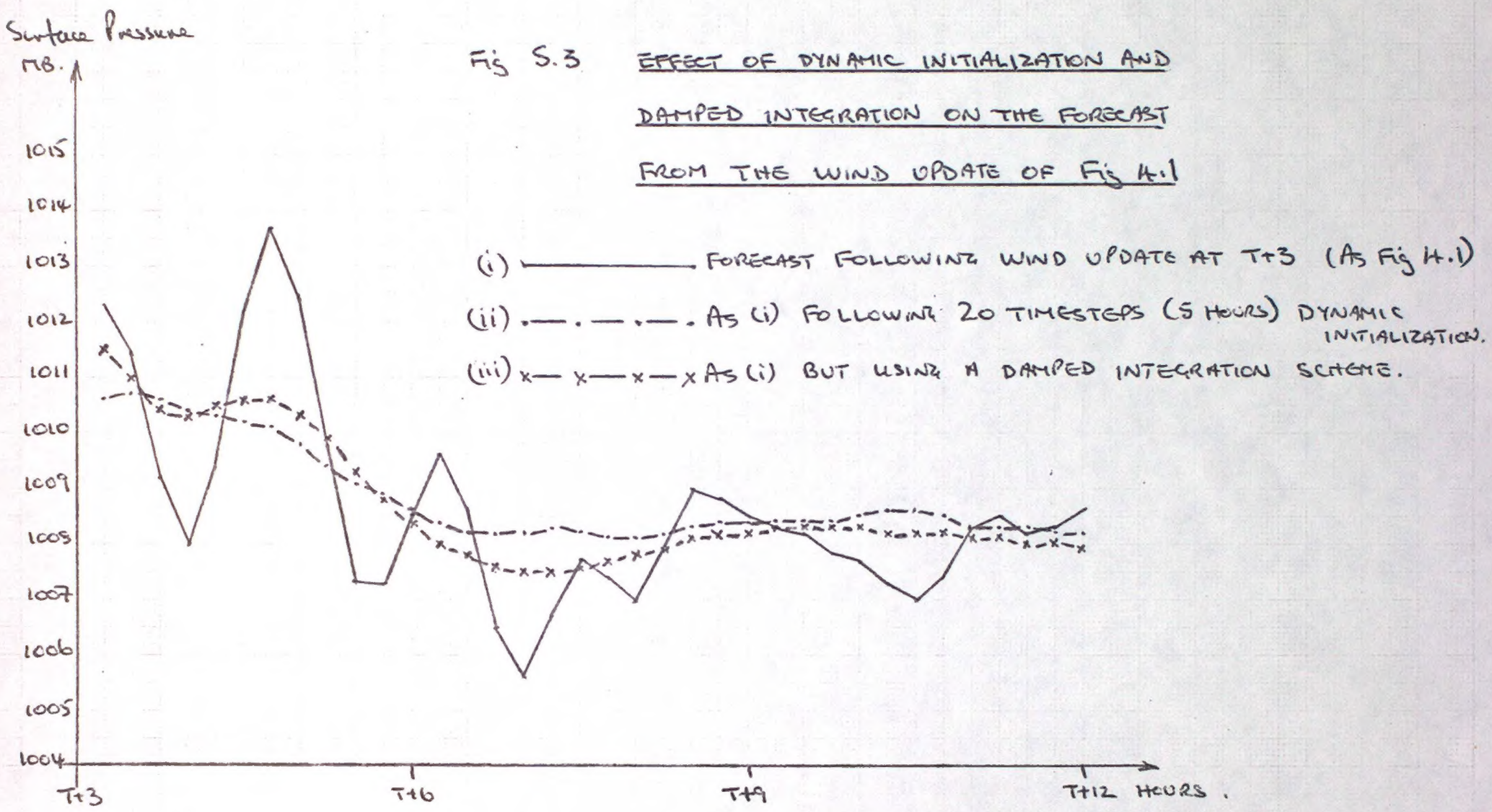
Fig 5.3 EFFECT OF DYNAMIC INITIALIZATION AND DAMPED INTEGRATION ON THE FORECAST FROM THE WIND UPDATE OF Fig 4.1